Chapter 2

Synthesis of Thiazolo[3,2-*a*]pyrimidine Molecules, In Vitro Cytotoxic Evaluation and Molecular Docking Studies

2.1 Introduction

Thiazolopyrimidine is a hybrid molecule containing of pyrimidine and thiazole heterocyclic rings is a fortunate moiety found in several natural products and many synthetic molecules. There are several bioactive thiazolopyrimidines that possess anticancer activity (**I-V**, **Fig 1**).[60]

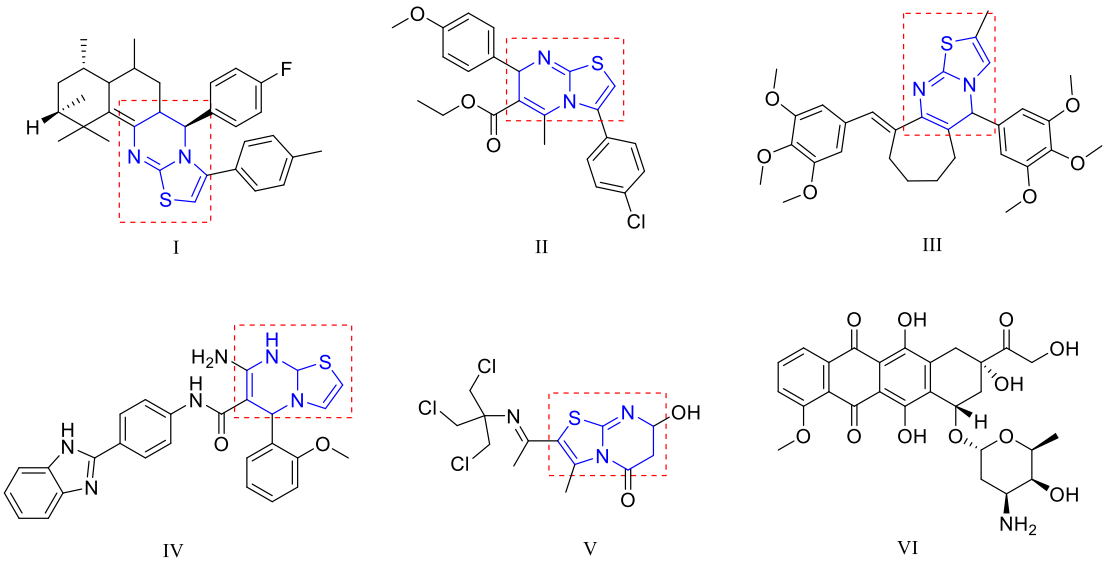

Fig 1. Bioactive fused thiazolopyrimidines (**I-V)** and structure of doxorubicin (**VI)**.

Many types of cancer are presently treated using the anticancer drug doxorubicin (**VI**, **Fig 1**). However, its usage has been restricted by elements including medication resistance, toxicity and congestive heart failure that have been documented in certain individuals.[61] Moreover, thiazolo[3,2-*a*]pyrimidine has appeared as a potential synthetic area in heterocyclic synthesis[62-68] due to its omnipresent applications as acetylcholinesterase inhibitor,[69] calcium antagonist,[70] cytotoxic agent,[71] antihypertensives,[72] antiproliferative,[73] Mycobacterium tuberculosis, O-acetyl serine sulfhydrylase inhibitor,[74] anticancer,[75,76] NK-2 antagonist,[77] antitubercular,[78] antitumor,[79] antiviral,[80] anti-inflammatory and antinociceptive[81] as well as in polymerization reactions as copolymer.[82,83]

Over the past two decades, there has been a wide interest increasing in the synthesis of hybrid molecules[84-86] and their assessment as a variety of powerful therapeutical and pharmacological agents. Hybrid molecules are stable molecular fusion of two biologically important molecules operating at separate sites, are a potential approach to treating complicated multifactorial disorders.[87-89] Two different molecular components are combined to form these "dual-acting compounds". Motivated by aforementioned activities of thiazolopyrimidines, we planned to synthesize some hybrid molecules comprising these two units. The newly developed molecules may be employed in very effective anticancer drugs since the hybridization of these two different biologically active molecules may have a synergic impact.

2.1.1 Synthetic approaches for substituted thiazolo[3,2-a]pyrimidine scaffold and its biological importance

R. Aggarwal[90] reported visible light driven synthesis of thiazolopyrimidine molecules and calculated the binding energy values with DNA and BSA. The reaction between diketone **1** with **2** under solvent-free condition in mortar and pestle formed the brominated diketone molecule **3** to which the tetrahydropyrimidine **4** molecule was added in ethanol and kept it under a 27 W visible light source or refluxed for appropriate time to form the fused thiazolopyrimidine molecule **5** in good yield **(Scheme 2.1)**.

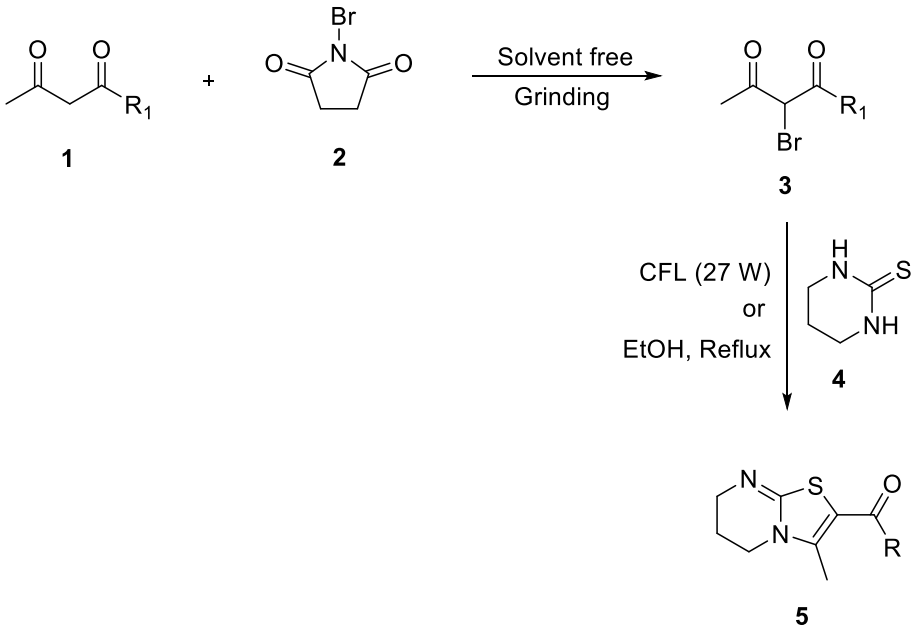

Scheme 2.1

U. Bhadraiah and co-workers[91] reported thiazolopyrimidine analogues and studied its antimicrobial properties. The reaction of phenylthiazole **6** with acetyl acetone **7** and various substituted benzaldehyde **8** in acetonitrile containing PTSA at reflux temperature formed the fused thiazolopyrimidine molecule **9**. Docking studies were also carried out with enzyme DNA gyrase to study the various docking poses. The synthesized molecules showed moderate to excellent antibacterial and antifungal activity against broad range of microorganisms **(Scheme 2.2)**.

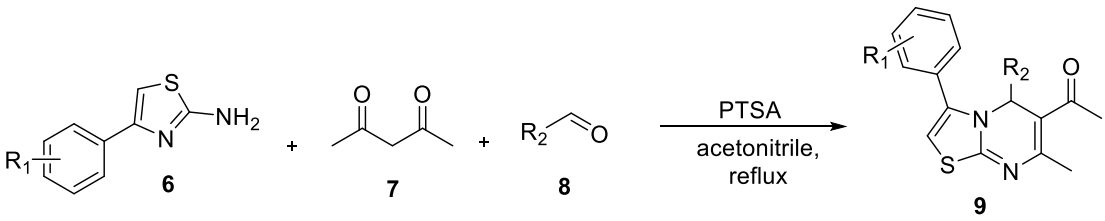

Scheme 2.2

A. Mohamed[92] reported on the synthesis of new thiazolopyrimidine molecules and screened them for anticancer activity. The reaction of molecule **10** with amino thiazole in butanol and DMSO formed the fused molecule **11** and the reaction with thiourea in ethanol with potassium hydroxide resulted in intermediate pyrido-pyrimidine molecule **12**, which was reacted with chloroacetic acid and bromo propanoic acid in presence of sodium acetate and refluxed in glacial acetic acid with acetic anhydride mixture to form molecules **13** and **14 (Scheme 2.3)**. Moreover, molecule **13** was reacted with diazonium salt and various aldehydes to form molecule **15** and **16 (Scheme 2.4)**.

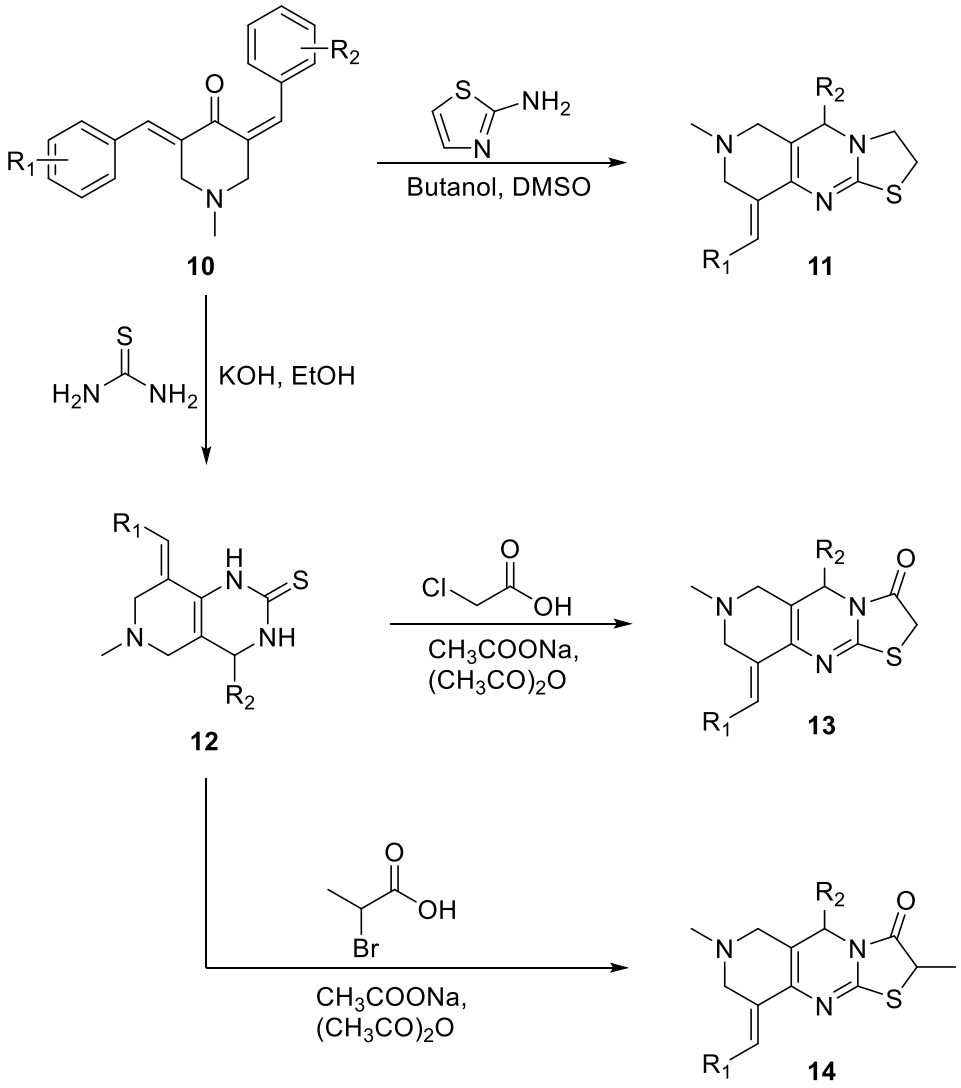

Scheme 2.3

The synthesized molecules were screened against a broad range of cancer cell lines and many of the molecules showed outstanding inhibition against various cell lines.

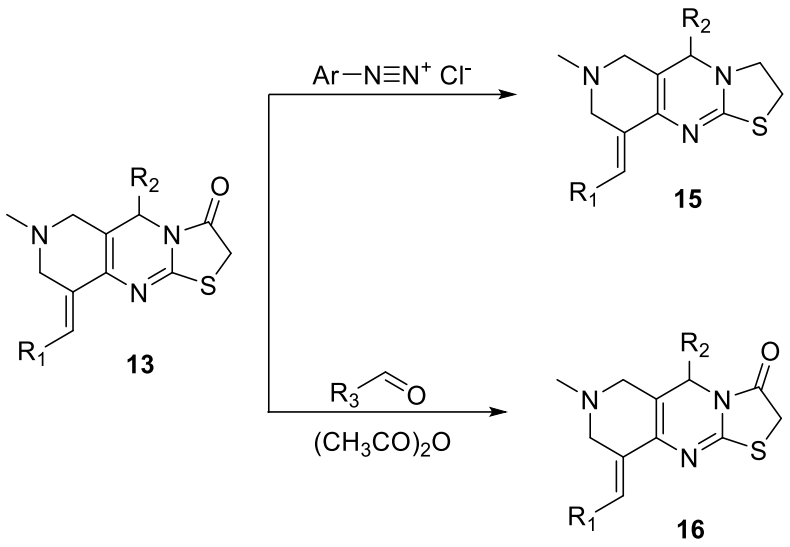

Scheme 2.4

D. Cai[93] reported on the synthesis of thiazolopyrimidine molecules and screened them for antibacterial and antituberculosis activity. The reaction between substituted uracil **17** with a derivative of phenacyl bromide in DMF containing potassium carbonate formed the intermediate molecule **18**, which was cyclized through reflux in concentrated sulphuric acid to form the thiazolopyrimidine molecule **19** and a nitro derivative was further reacted with ferrous to form molecule **20**. The synthesized molecules showed good activity against gram-positive bacteria and the presence of benzoyl amido substitution in the ring showed a greater increase in antimicrobial and antituberculosis activity **(Scheme 2.5)**.

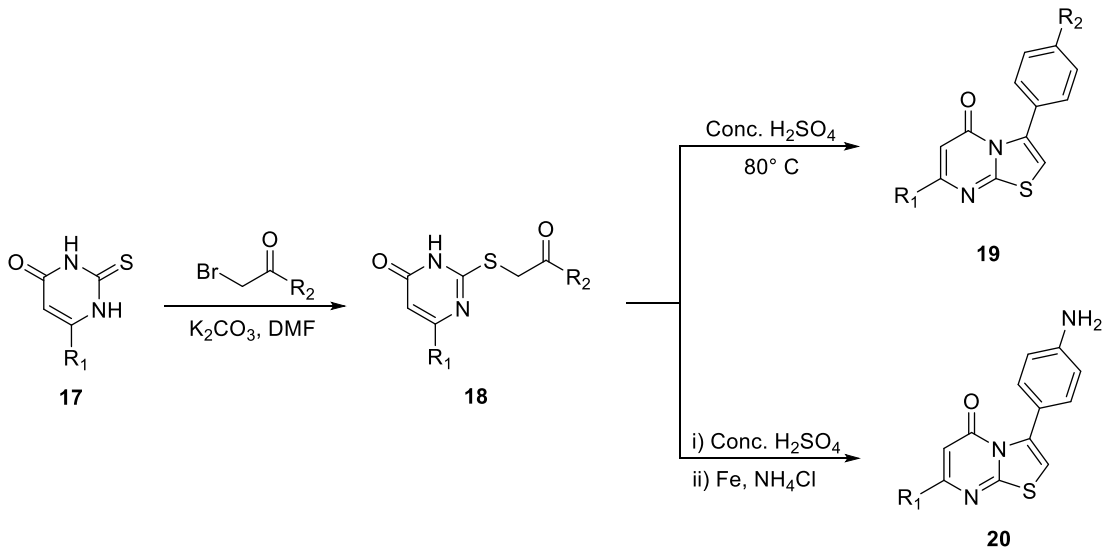

Scheme 2.5

Wang[94] reported on the synthesis of pyrazole-thiazolopyrimidine molecules and evaluated them for antiproliferative activity. The phenylpyrazole molecule **21** was converted to an aldehyde **22** molecule through a reaction with DMF and phosphorus oxychloride. Then molecule **22**, thiourea **23** and ethyl acetoacetate **24** was refluxed in ethanol containing catalytical amount of hydrochloric acid to form pyrimidine molecule **25** which was reacted with chloroacetic acid and aldehyde to form thiazolopyrimidine **26** molecule. Some of the synthesized molecules showed high potency and induced apoptosis of MGC-803 cells **(Scheme 2.6)**.

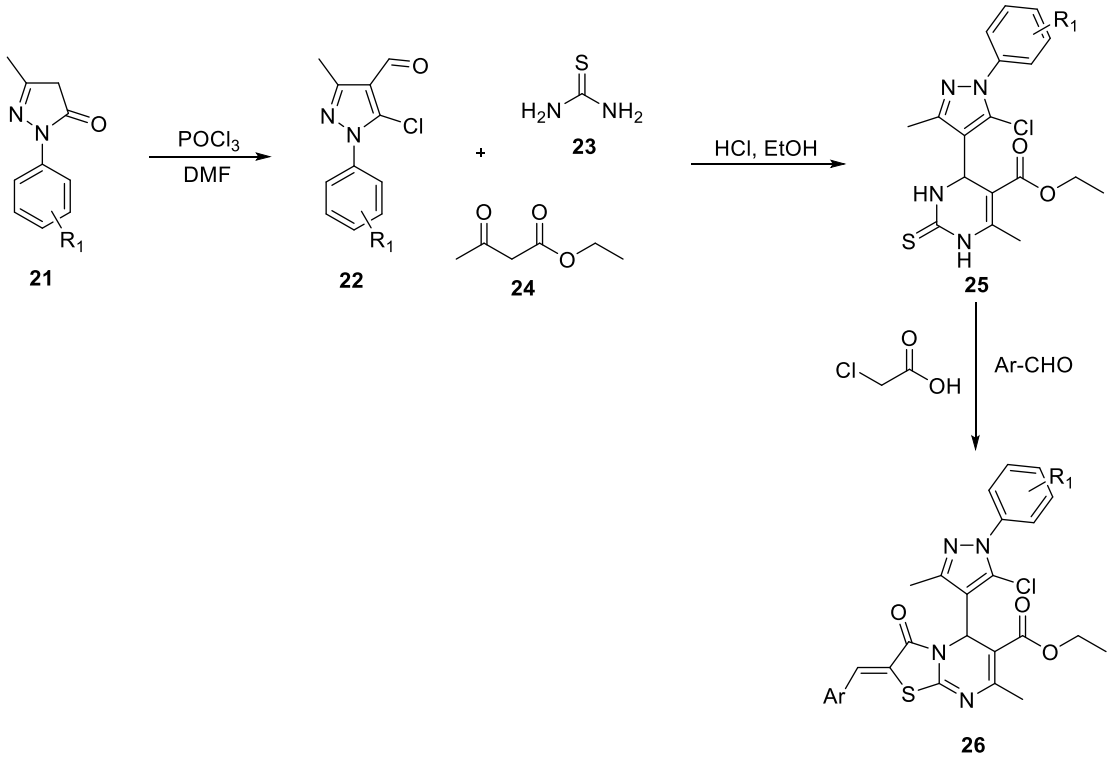

Scheme 2.6

H. Alzahrani[95] reported synthesis of fused thiazolopyrimidine molecules via reaction of chloro thiazolopyrimidine **27** molecule with dihydropyridine carbonitrile to form thienopyridine molecule **28** to which various substituted benzaldehydes were attached to form molecule **29** in moderate yield. The synthesized molecules showed good to excellent anticancer activity against MCF-7 cell line **(Scheme 2.7)**.

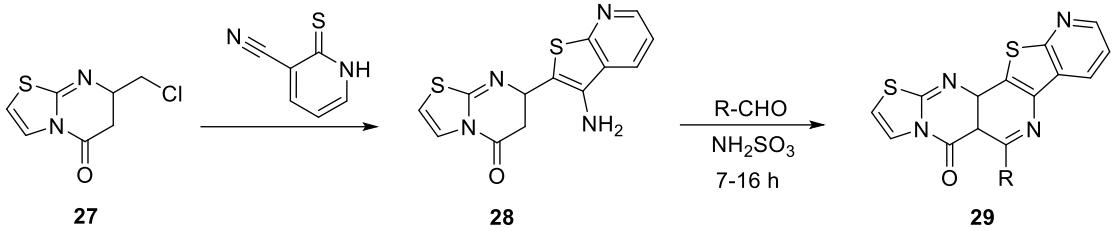

27 28 29

Scheme 2.7

A. Darehkordi[96] reported trichloro thiazolopyrimidine molecule synthesis via reacting pyrimidine thione **30** molecule with pentachloro pyridine **31** in acetonitrile containing potassium carbonate formed new thiazolopyrimidine molecule **32 (Scheme 2.8)**.

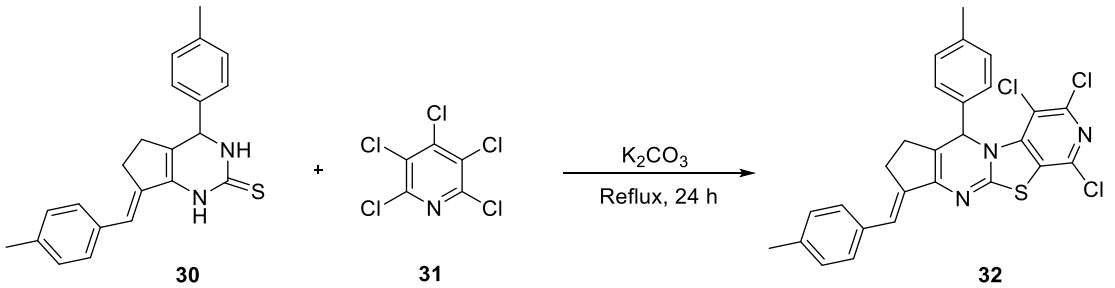

30 31 32

Scheme 2.8

S. Borthakur[97] reported on the synthesis of thiazolopyrimidine and studied its antifungal activity. The reaction between phenylthiazole **33** and arylidene malononitrile **34** derivative in propanol using sodium hydroxide as a catalyst formed novel thiazolopyrimidine molecules **35**. The synthesized molecules were screened against *Rhizoctonia solani* and *Drechslera orazae* fungal pathogens which causes diseases on rice plants. The results of the antifungal activity showed mild to moderate inhibitory activity **(Scheme 2.9)**.

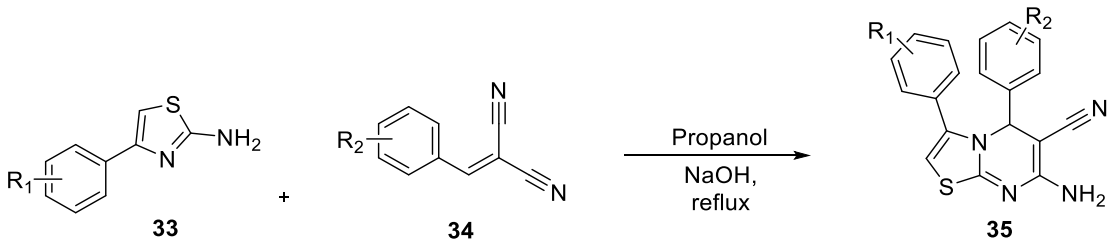

33 34 35

Scheme 2.9

D. Egorov[98] reported a new synthesis of phosphorylated thiazolopyrimidine molecules via reaction of tetrahydropyrimidine **36** molecule with diethyl chloroethynyl

phosphonate **37** in acetonitrile containing catalytic amount of potassium carbonated resulted in thiazolopyrimidine molecule **38 (Scheme 2.10)**.

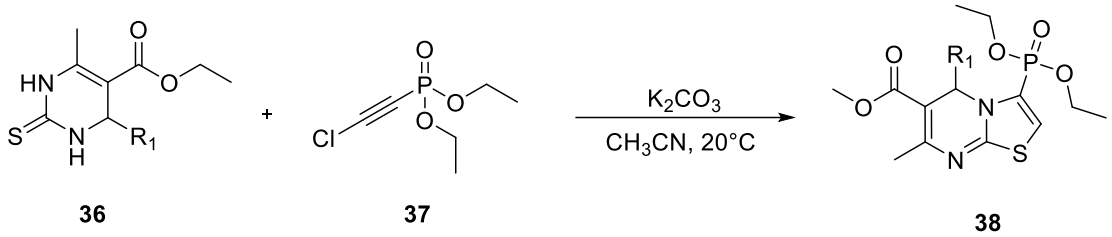

36 **37** **38**

Scheme 2.10

M. Buddh[99] reported the synthesis of new thiazolo[3,2-α]pyrimidine molecules and examined its bioactivity. The reaction between acetoacetanilide derivative **39**, thiourea **40** and substituted benzaldehyde **41** in ethanol at reflux temperature formed pyrimidine **42** molecule. Furthermore, pyridine molecule was cyclized via reaction with chloro acetic acid and acetic anhydride and attached substituted aldehyde to active methylene to form novel molecules of thiazolopyrimidines **43**. The synthesized molecules were screened for antibacterial activity against a range of gram-positive and gram-negative bacteria **(Scheme 2.11)**.

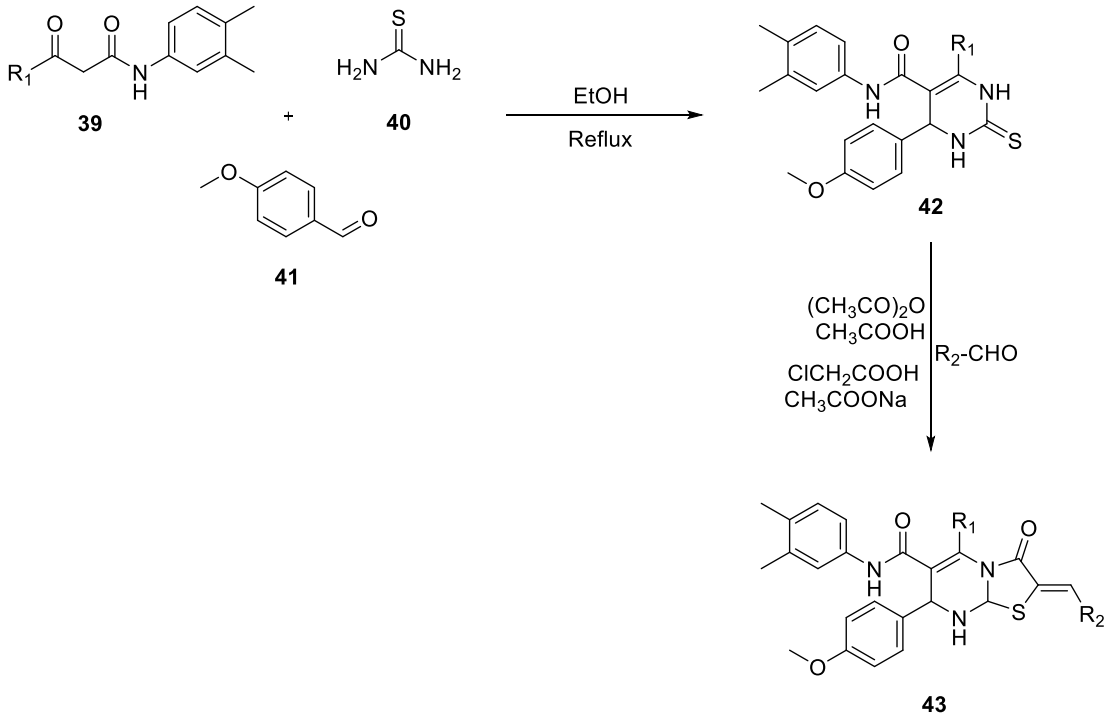

39 **40** **41** **42** **43**

Scheme 2.11

M. Esmaeilinezhad[100] reported the synthesis of chroman fused thiazolopyrimidine molecule under solvent-free conditions using ionic liquid. The reaction between dimedone **44**, substituted benzaldehyde **45** and thiazolopyrimidine **46** heated with an acid catalyst in neat condition gave a fused chroman thiazolopyrimidine **47** molecule in good yields. The synthesized molecules were expected to be used of pharmacological interest **(Scheme 2.12)**.

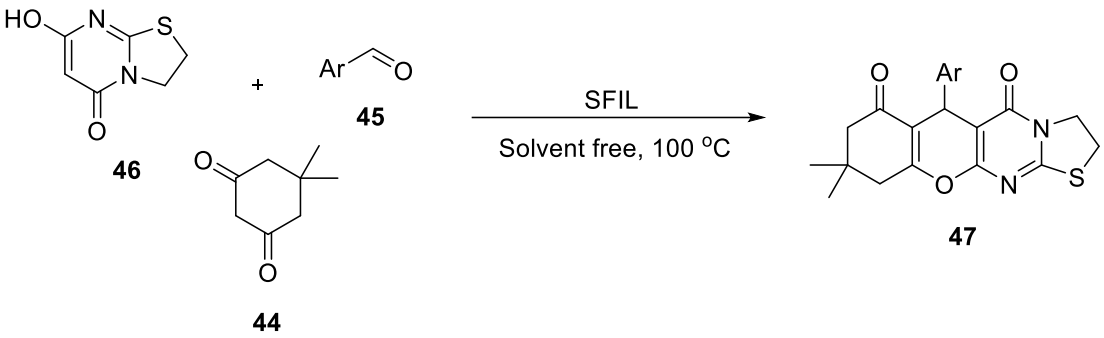

Scheme 2.12

A. Aly[101] reported synthesis of thiazolopyrimidine via reacting pyrimidine thiol **48** molecule with chloroacetic acid **49** in the presence of ammonium acetate formed thiazolopyrimidine **50** molecule. Furthermore, the reaction of molecule **50** with various aldehydes formed molecule **51** which was cyclized through reaction with hydroxylamine in pyridine to form thiazolopyrimidine-isooxazole molecule **52**. The synthesized molecules were screened for antibacterial and antifungal activity **(Scheme 2.13)**.

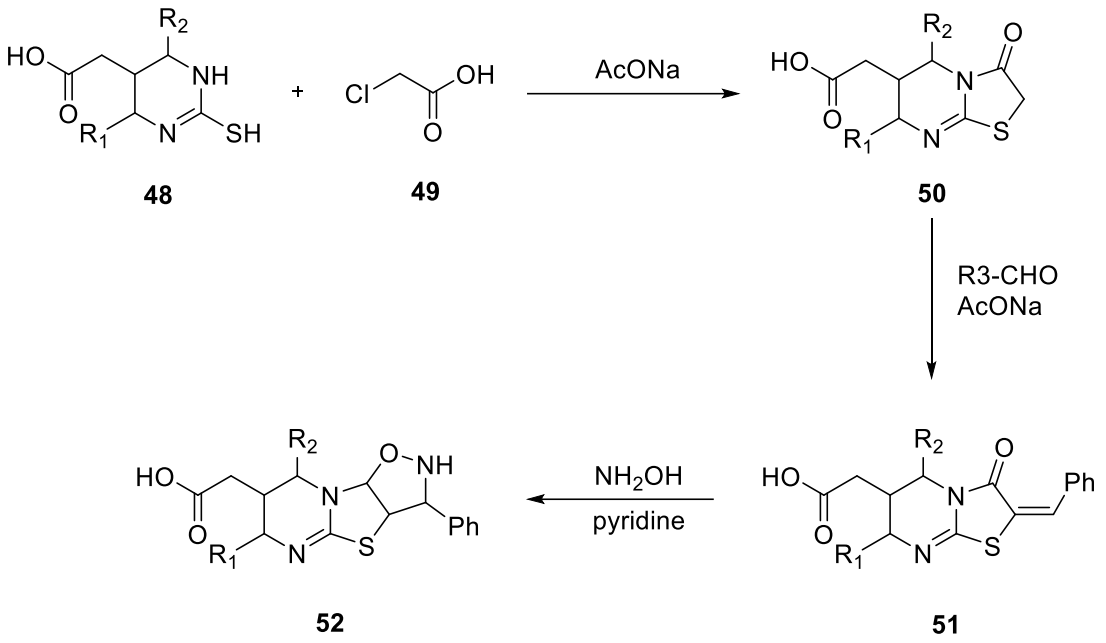

Scheme 2.13

H. Sayed[102] reported triazole-thiazolopyrimidine molecules synthesis from pyrimidine **53** molecule reacted with bromoacetyl bromide in DMF containing sodium hydroxide resulted in thiazolopyrimidine molecule **55**. Moreover, molecule **55** was reacted with thionyl chloride followed by sodium azide to form azide molecule **56 (Scheme 2.14)**, which was reacted with various molecules such as ethyl acetoacetate, ethyl cyanoacetate, malononitrile and diethyl malonate to form respective molecules **57**, **58**, **59** and **60** which holds 1,2,3-triazole and thiazolopyrimidine in its core structure **(Scheme 2.15)**. The synthesized molecules showed promising antimicrobial activity.

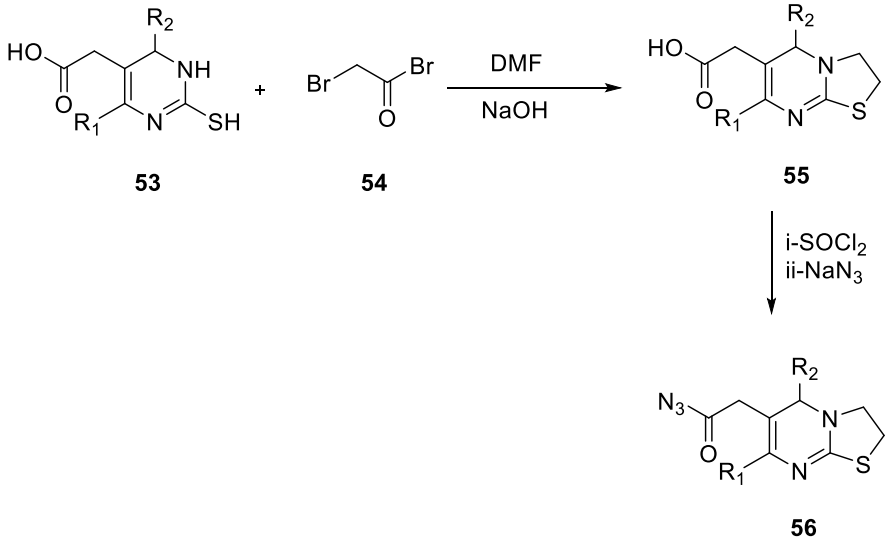

Scheme 2.14

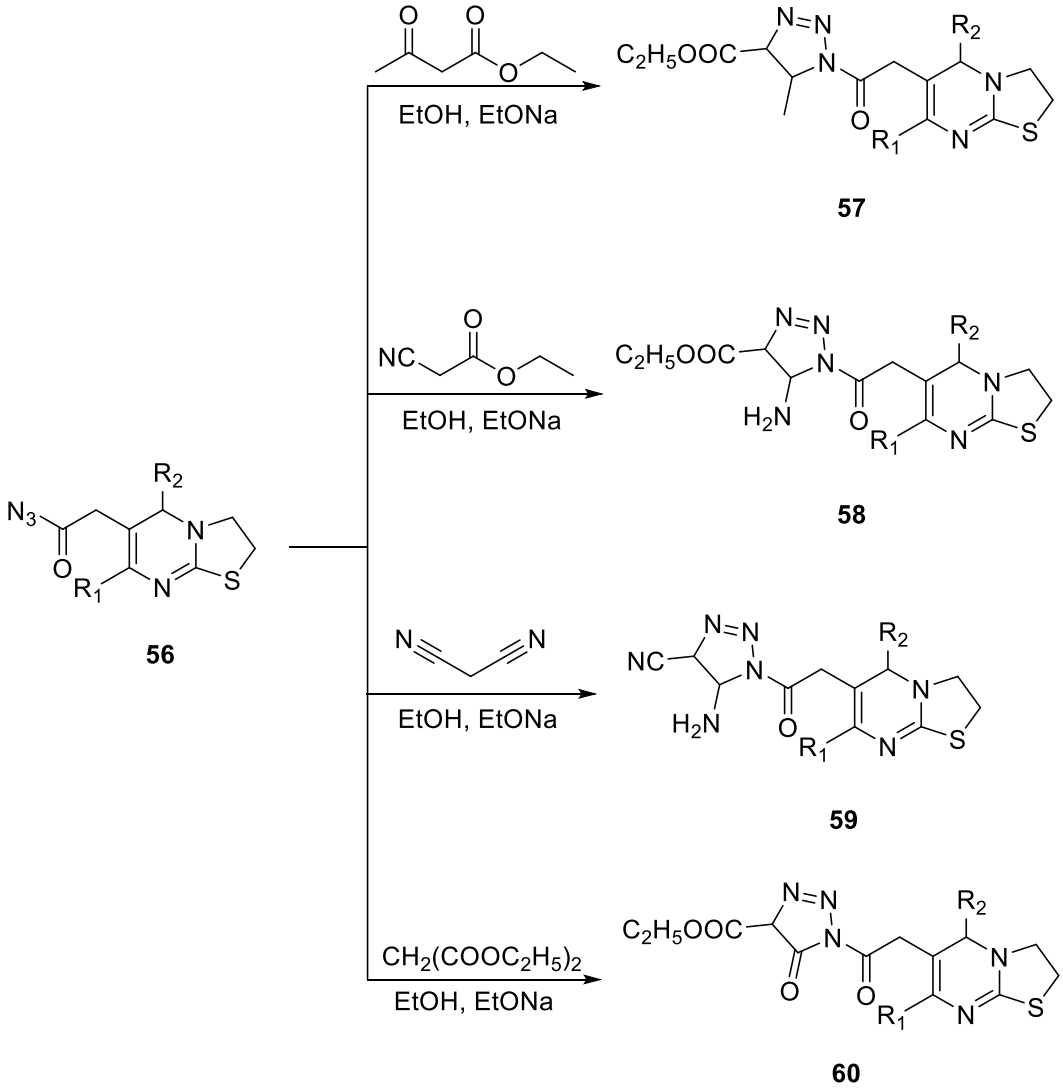

56 **57** **58** **59** **60**

Scheme 2.15

2.2 Results and Discussion

To find a novel anticancer molecule and the synthesis of different heterocyclic molecules, here, we report ten newly synthesized molecules with thiazolo[3,2-*a*]pyrimidine in their main structure. The compounds **4a-t** were elucidated through inspecting their spectroscopic data like ^{1}H-NMR, ^{13}C-NMR, FTIR and mass spectroscopy. In the first step, 3-oxo-*N*-arylbutanamide and *N*-bromosuccinimide reacted at ambient temperature to get 2-bromo-3-oxo-*N*-arylbutanamide. Then thiourea was added for ring closure to obtain 2-amino-*N*-aryl-4-methylthiazole-5-carboxamide **3a-t.**

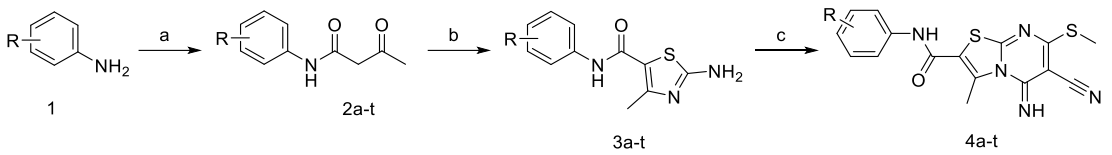

Scheme 1: Reagents and Conditions: (a) Ethyl acetoacetate, KOH, Reflux, 24 hr (b) NBS, Thiourea, MeOH, Reflux, 4 hr (c) 2-bis(methylthio)methylene malononitrile, K_2CO_3, DMF, Reflux, 30 min.

Then, compound **3a-t** was reacted with 2-bis(methylthio)methylene malononitrile to obtain novel and highly functionalized thiazolo[3,2-*a*]pyrimidine **4a-t** derivatives as appear in **Scheme 1**. The ^{1}H-NMR graph of compounds presented that 4-methyl thiazole protons were detected at s 2.20–2.57 ppm (CH_3) as a singlet, at s 2.94–3.05 ppm (SCH_3) for pyrimidine thiomethyl protons which were singlet peaks. The aromatic region was seen between 6.94–7.83 ppm. A smaller singlet peak seen at s 9.03–10.64 ppm (NH) indicated the pyrimidine imine proton. Acetamide protons were observed at s 9.81–10.80 ppm (NH) as a singlet. To optimize the reaction conditions for the synthesis of compound **4a-t**, various bases such as anhydrous potassium carbonate and triethylamine, were utilized in respective solvents, such as methanol, ethanol, tetrahydrofuran and acetonitrile. As a result, we found that the reaction of **3a-t** with 2-bis(methylthio)methylene malononitrile was faster and afforded the thiazolo[3,2-*a*]pyrimidine **4a-t** in good yield in the presence of potassium carbonate and DMF. Furthermore, the reaction of thiazolo[3,2-*a*]pyrimidine with different primary and secondary amines or phenols was not promising to yield substituted thiazolo[3,2-*a*]pyrimidine derivatives because of the poor reactivity of SMe, so maybe oxidation of the sulfides to sulfones can transfer it into good leaving group thus allowing good

reactivity and further derivatives of thiazolo[3,2-*a*]pyrimidine can be produced. We have also observed that the reaction of thiazolo[3,2-*a*]pyrimidine with hydrazine hydrate and phenyl hydrazine yielded a mixture of cyclized and noncyclized products. Due to high nitrogen content, lipophobicity and poor solubility in a variety of solvents, the purification of the product was not possible. The one-pot reaction of acetoacetanilide, *N*-bromosuccinimide followed by thiourea and further addition of 2 bis(methylthio)methylene malononitrile to obtain cyclized thiazolo[3,2-*a*]pyrimidine was not clean and did not yield the desired product.

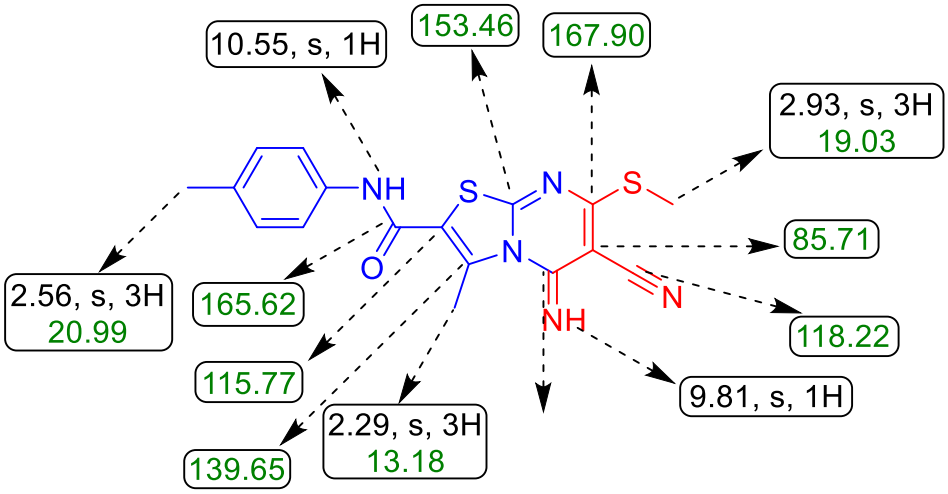

Fig 1. Selected ^{1}H (black) and ^{13}C NMR (green) of **4b.**

2.2.1 Optimizing reaction condition

Primarily, the experiment was done without using any solvent or catalyst at 90°C, but the outcome was none (**Table 1**, entry 1). Therefore, the next reaction was executed using water as a solvent and without a base at ambient temperature for 1 hour but product formation did not occur (entry 2). So, with the addition of potassium carbonate, the mass was refluxed for 1 hour but the result was again disappointing, no product formation was seen (entry 3). Then triethylamine was used as a base and acetone as solvent refluxed for 1 hour, leading to 12% of the product (entry 4) and 10% product formation when potassium carbonate was used as a base (entry 5). Reaction state was then changed regarding the solvent using methanol and triethylamine as a base. This resulted in the product being obtained in 10% yield (entry 6) and as a base when potassium carbonate was used yield was 12% (entry 7). Further optimization of the

reaction was done by using ethanol as a solvent and triethylamine as a base. Then the mass was refluxed for 1 hr and product was obtained in 38% yield (entry 8) and 43% yield was obtained when potassium carbonate was used as a base (entry 9). Subsequently, the use of tetrahydrofuran as a solvent and triethylamine as a base produced a product of 32% (entry 10) while the use of potassium carbonate produced a yield of 38% (entry 11). Surprisingly, when using acetonitrile as a solvent and triethylamine as a base, the yield was 45% (entry 12) and when potassium carbonate was used as a base, 59% yield (entry 13) was archived.

Table 1. Optimization of the Reaction Conditions.

Entry	Solvent	Base	Temp. (°C)	Yield (%)	Purification Necessary/ By-product formation
1	No Solvent	-	90	-	-
2	H_2O	-	rt	-	-
3	H_2O	K_2CO_3	Reflux	-	-
4	Acetone	Et_3N	Reflux	12	Yes
5	Acetone	K_2CO_3	Reflux	10	Yes
6	MeOH	Et_3N	Reflux	10	Yes
7	MeOH	K_2CO_3	Reflux	12	Yes
8	EtOH	Et_3N	Reflux	38	Yes
9	EtOH	K_2CO_3	Reflux	43	Yes
10	THF	Et_3N	Reflux	32	Yes
11	THF	K_2CO_3	Reflux	38	Yes
12	MeCN	Et_3N	Reflux	45	Yes
13	MeCN	K_2CO_3	Reflux	59	Yes
14	DMF	Et_3N	Reflux	62	Yes
15	**DMF**	**K_2CO_3**	Reflux	**95**	**No**

When N, N-dimethylformamide was used with triethylamine, this yielded a 62% yield (entry 14), but when potassium carbonate as a base reaction mixture was heated to reflux for 30 min the resultant yield was 95% (entry 15). This variation did not lead to the formation of by-products and gave an excellent yield with high purity. It was clearly

observed that, while triethylamine overall yield was low compared to potassium carbonate. Solvents such as methanol and acetone reduced the yield of product, respectively (entry 2 and 3), using water as a green solvent, the experiment did not continue smoothly, maybe because of the poor solubility of the reactants in water. With the optimized reaction environments, the technique was used to produce novel ten thiazolo[3,2-*a*]pyrimidine **4a-t** molecules (**Table 2**).

Synthesized molecules **4a-t** were further investigated for molecular docking to determine the binding affinity of the molecules.

2.2.2 Physicochemical Properties

Table 2. Physicochemical Characteristics of the Thiazolo[3,2-*a*]pyrimidine Molecules 4a-t

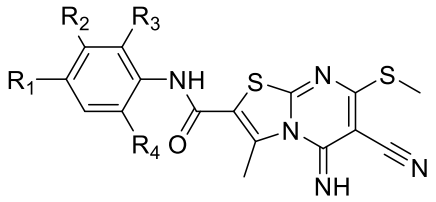

Entry	R^1	R^2	R^3	R^4	Molecular weight	Molecular formula	Yield (%)	Melting point (°C)
1	OCH_3	H	H	H	385.46	$C_{17}H_{15}N_5O_2S_2$	83	213-215
2	CH_3	H	H	H	369.46	$C_{17}H_{15}N_5OS_2$	91	226-228
3	H	H	H	H	355.43	$C_{16}H_{13}N_5OS_2$	72	201-203
4	H	Cl	H	H	389.88	$C_{16}H_{12}ClN_5OS_2$	67	216-218
5	CH_3	H	CH_3	H	383.49	$C_{18}H_{17}N_5OS_2$	87	242-244
6	Cl	H	H	H	389.88	$C_{16}H_{12}ClN_5OS_2$	89	230-232
7	H	H	CH_3	CH_3	383.49	$C_{18}H_{17}N_5OS_2$	65	238-240
8	F	H	H	H	373.42	$C_{16}H_{12}FN_5OS_2$	61	237-239
9	Br	H	H	H	434.33	$C_{16}H_{12}BrN_5OS_2$	86	248-250
10	H	H	OCH_3	H	385.46	$C_{17}H_{15}N_5O2S_2$	90	212-214
11	H	CF_3	H	H	423.43	$C_{17}H_{12}F_3N_5OS_2$	62	240-242
12	H	OCH_3	H	H	385.46	$C_{17}H_{15}N_5O_2S_2$	78	207-209
13	H	H	H	F	473.42	$C_{16}H_{12}FN_5OS_2$	71	233-235
14	F	Cl	H	H	407.87	$C_{16}H_{11}ClFN_5OS_2$	75	239-241
15	CH_3	CH_3	H	H	383.49	$C_{18}H_{17}N_5OS_2$	82	247-249
16	H	H	Cl	Cl	424.32	$C_{16}H_{11}Cl_2N_5OS_2$	85	221-223
17	Cl	Cl	H	H	424.32	$C_{16}H_{11}Cl_2N_5OS_2$	80	227-229
18	H	F	H	H	373.42	$C_{16}H_{12}FN_5OS_2$	63	232-234
19	H	Br	H	H	434.33	$C_{16}H_{12}BrN_5OS_2$	87	244-246
20	H	CH_3	H	H	369.46	$C_{17}H1_5N_5OS_2$	82	220-222

2.2.3 Molecular docking with α-amylase

Seeing the excellent in vitro outcomes, molecular docking was performed on the synthesized molecules to study both in vitro and in silico outcomes. As the target receptor topoisomerase II alpha was used. Molecular docking study was executed to study the affinity of the synthesized molecules via Autodock Vina. The crystal structure of Topoisomerase II alpha was downloaded from Protein Data Bank with PDB id 1ZXM. The docking results of synthesized molecule displayed hydrogen bond with several amino acid. The main bonding amino acids were Arg241, Lys321, Lys168, Tyr73, Tyr82, Arg242, Glu379, Gln59 and Arg 324. The prepared 3D molecule structures were energy minimized and utilized for docking studies. All newly prepared molecules were subjected to docking.

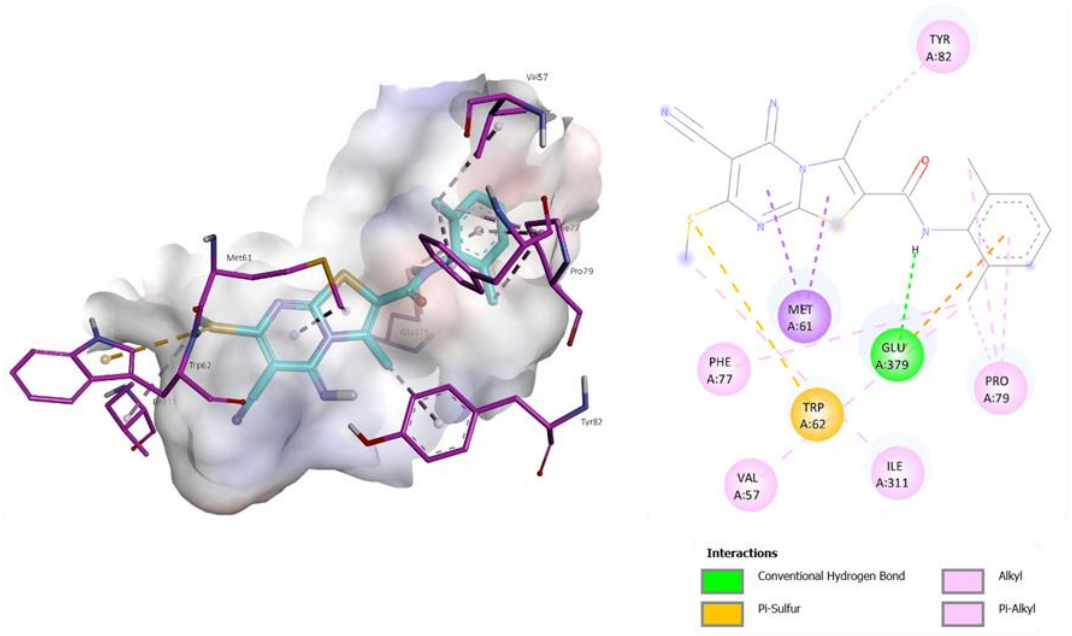

Fig 4. Docking pose of **4e** with topoisomerase-II

Table 4 shows the docking score with binding energy and active site residues with doxorubicin as standard. All prepared molecules exhibited decent binding energy with the target varying from -7.9 to -8.7 kJ mol^{-1}. Among all the molecules, molecule **4e** had best docking value of -8.7 to the standard doxorubicin. Amongst the experimented molecules, the nitrile group of compound **4a** formed H-bonding with Arg B:241 and Lys B:321, nitrile group also shows H-bonding with Lys A:168 in compound **4b**. In compound **3c,** two hydrogen bonds formed with Tyr B:73 and Arg B:241. Compound

4d did not form any H-bond, but formed a conventional and van der waals bond with Trp B: 62 and Lys B:83. Imine hydrogen from thiazolopyrimidine **4e** formed the H-bond with the amino acid Tyr B:82, Compound **4e** also formed the pi sulfur bond with Trp B:62 and alkyl and pi-alkyl bonds with Pro B:79, Val B:57, Phe B: 77 and Met B:61 shown in **Fig. 4** with a docking score of -8.7 compared to standard doxorubicin. Compound **4f** formed two hydrogen bonds with nitrile and ketone group with amino acids Arg B:242 and Trp B:62, Amide hydrogen of compound **4g** formed H-bond with amino acid Glu A:379 having a docking score -8.6. Compound **4g** also formed pi-anion bond with Glu A:379, pi-sigma bond with Met A:61, pi-sulfur bond with TrpA:62, alkyl and pi-alkyl bond with Val A:57, Phe A:77, Ile A:311 Pro A:79.

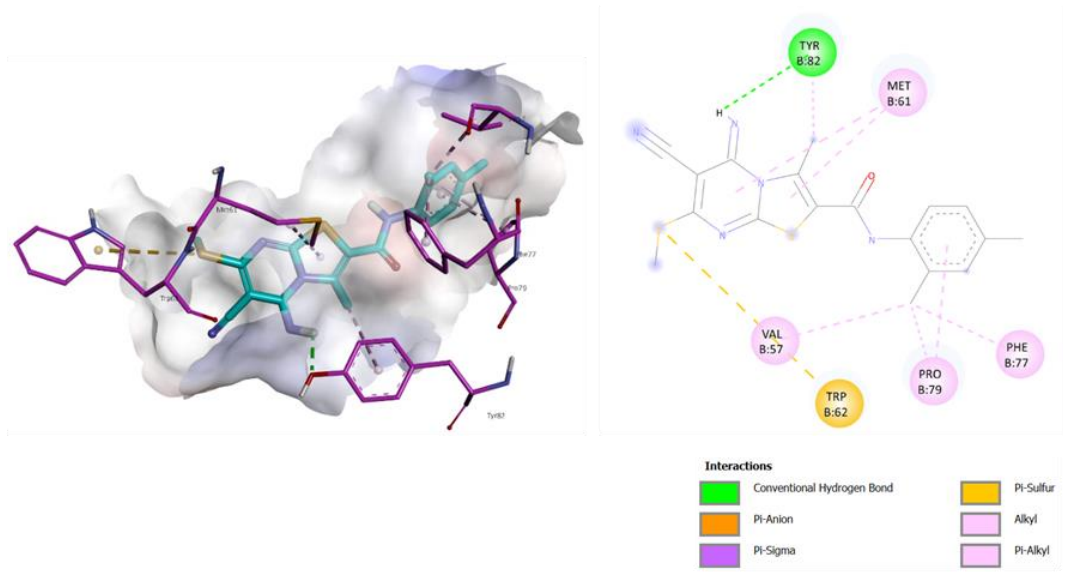

Fig 5. Docking pose of **4g** with topoisomerase-II

Compound **4h** formed two hydrogen bonds with Gln B:59 and Arg B:241. compound **4i** formed H-bond with Arg B:242. Compound **4j** formed H bonding with Arg A: 324, Glu B: 379. The docking studies revealed that the thiazolopyrimidine having CH_3 group as a substitution on the aryl ring in the molecule **4e** and **4g** displayed excellent inhibitory activity and interface with the target enzyme.

2.3 Cytotoxic assessment

The outcomes displayed in **Table 3** showed that among the thiazolopyrimidine molecules, few of the molecules assessed showed excellent anticancer activity in different cancer cell lines. Cytotoxic assessment data is shown in **Table 3 and** it was discovered that between the prepared thiazolopyrimidines. Some of the molecules examined showed moderate to good anticancer action opposed to different cancer units. In particular, molecule **4g** exhibited outstanding activity on A549 (3.1 ± 0.4), compound **4f** displayed good activity on MCF-7 (6.8 ± 0.7). Compound **4g** also showed (9.8 ± 0.4) good results in HeLa. Compound **4c** having phenyl ring displayed less activity against screened cell lines. Compounds **4e** and **4g** of thiazolopyrimidine with methyl substitutions on the phenyl ring showed excellent activity in cell lines. These outcomes discovered that molecules with methoxy and halogen substitute on thiazolopyrimidine exhibited powerful anticancer activity. Therefore, these outcomes could be noteworthy in the development of potent and harmless anticancer molecules.

Table 3. IC_{50} of the Synthesized Molecules against Cancer Cell Lines

Sample code	IC_{50} in µM					
	A549		MCF-7		HeLa	
	24 h	48 h	24 h	48 h	24 h	48 h
4a	10.2 ± 0.4	8.4 ± 0.3	17.4 ± 0.4	15.3 ± 0.2	15.3 ± 0.5	12.5 ± 0.5
4b	7.4 ± 0.3	6.3 ± 0. 2	15.7 ± 0.3	12.3 ± 0.2	17.3 ± 0.5	14.5 ± 0.3
4c	12.3 ± 0.3	10.5 ± 0.6	12.1 ± 0.3	10.1 ± 0.5	22.2 ± 0.3	20.1 ± 0.3
4d	15.5 ± 0.2	12.4 ± 0.4	9.3 ± 0.5	7.3 ± 0.6	19.7 ± 0.2	15.4 ± 0.2
4e	6.4 ± 0.2	3.2 ± 0.5	18.3 ± 0.4	14.2 ± 0.3	14.1 ± 0.4	10.3 ± 0.5
4f	13.5 ± 0.4	10.3 ± 0.3	9.5 ± 0.4	6.8 ± 0.7	15.8 ± 0.3	11.2 ± 0.7
4g	6.1 ± 0.3	3.1 ± 0.4	20.2 ± 0.2	17.5 ± 0.4	13.2 ± 0.6	9.8 ± 0.4
4h	10.1 ± 0.6	9.1 ± 0.3	9.3 ± 0.3	7.1 ± 0.5	14.6 ± 0.5	10.9 ± 0.1
4i	12.7 ± 0.4	10.2 ± 0.5	10.8 ± 0.4	8.3 ± 0.3	16.8 ± 0.2	14.4 ± 0.4
4j	11.5 ± 0.2	8.5 ± 0.3	17.9 ± 0.2	14.4 ± 0.6	16.2 ± 0.3	14.1 ± 0.3
Doxorubicin	0.9 ± 0.03	0.7 ± 0.04	1.4 ± 0.2	0.9 ± 0.02	0.6 ± 0.05	0.4 ± 0.03

The IC_{50} value was calculated from the dose response curve. The values (µM) denote the average ± SD of three different assessments. Doxorubicin was utilized as a positive control.

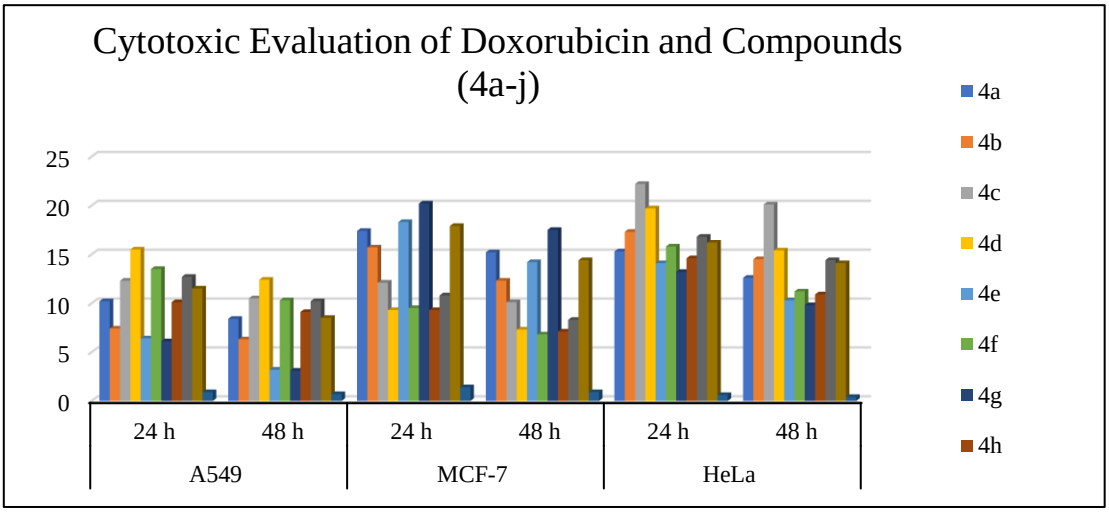

Fig 3. Cytotoxicity evaluation of doxorubicin and compounds **4a-j** against HeLa, MCF-7 and A549 cancer cell lines.

❖ Structure of ethyl 6-cyano-5-imino-3-methyl-7-(methylthio)-5*H*-thiazolo[3,2-*a*]pyrimidine-2-carboxylate (2)

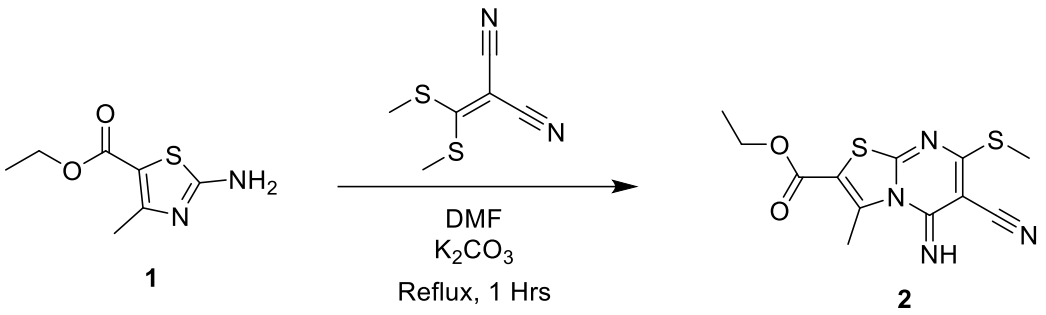

❖ Procedure for the development of single crystals.

In this study, pure single spot compound (on TLC) was dissolved in DMF and heated until it dissolved. A small amount of charcoal was added to decolorize. The solution was then heated to boiling and filtered immediately while hot in a corkable 50 ml conical flask with whatmann filter paper. The bottle was corked and kept for 45 days. Thus, the crystals grown by the slow evaporation of the solvent were isolated and washed with chilled methanol. The structure of 6-cyano-5-imino-3-methyl-7-(methylthio)-5*H*-thiazolo[3,2-*a*]pyrimidine-2-carboxylate has been characterized by IR, ^{1}H & ^{13}C NMR and mass spectral studies.

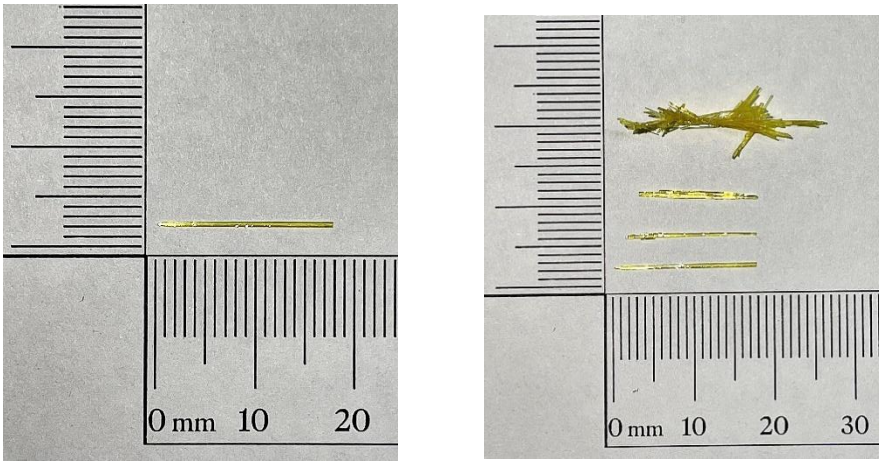

Fig 1. Photographs of the grown crystal of Compound 2

Good quality single crystals with maximum dimension 1 mm X 18 mm were obtained. **Fig 1.** show the types of crystals grown. The crystals were yellow in colour.

2.4 Conclusion

In conclusion, a series of novel *N*-aryl-6-cyano-5-imino-3-methyl-7-(methylthio)-5*H*-thiazolo[3,2-*a*]pyrimidine-2-carboxamide has been synthesized starting from various 2-amino-*N*-aryl-4-methylthiazole-5-carboxamide with excellent yields. The important features of this reaction technique are novel, easy and less time consuming. The chemical structures of the molecules were characterized by their spectral data such as FTIR, ^{1}H NMR, ^{13}C NMR and MS. Molecules were assessed for cytotoxic activity against human breast carcinoma cell line (MCF-7), human lung adenocarcinoma cell line (A549) and human cervical cancer cell line (HeLa). Tested molecules **4a-j** showed moderate to excellent anticancer activity against various cell lines. Compound **4g** with IC_{50} value of 3.1 ± 0.4 µM against A549, compound **4f** with IC_{50} value of 6.8 ± 0.7 µM against MCF-7 and in HeLa cell line compound **4g** with IC_{50} value of 9.8 ± 0.4 µM showed best cytotoxic results. Moreover, a molecular docking study was carried out for synthesized molecules **4a-j** against topoisomerase-II via utilizing the Autodock technique. The docking outcomes of molecule **4b**, **4e** and **4g** showed a good cytotoxic activity.

2.5 Experimental Section

Melting points were determined on an electrothermal device using open capillaries and are uncorrected. Thin-layer chromatography was performed on precoated silica gel 60 F254 (Merck), the compounds were visualized with UV light at 254 nm and 365 nm or with iodine vapor. The IR spectra were recorded on a Shimadzu FT-IR spectrometer using the ATR technique. ^{1}H and ^{13}C NMR spectra were recorded on a Bruker AVANCE III (400 MHz) spectrometer in DMSO-d_6 or $CDCl_3$. Chemical shifts are expressed in δ ppm downfield from Tetramethylsilane (TMS) as an internal standard. Mass spectra were recorded using a direct inlet probe on Shimadzu GCMS QP2010 Ultra mass spectrometer. All reactions were carried out under an ambient atmosphere. All reagents were purchased from Loba, Molychem, SRL and CDH and used without further purification.

- **General process for the synthesis of acetoacetanilide (2a-t)**

Substituted amine (10 mmol) and ethyl acetoacetate containing catalytic amount of Potassium or sodium hydroxide lie (10%) in toluene was refluxed for approximately 24 hr. On completion of the reaction, the mass was evaporated under vacuum and the residue was crystallized from methanol or ethanol to get pure acetoacetanilide.

- **General process for the synthesis of thiazoles (3a-t)**

To a stirred solution of compound acetoacetanilide (10 mmol) **(2a-t)** in MeOH, *N*-bromosuccinimide (15 mmol) was added and stirred at room temperature for 30 min. To this reaction mass thiourea (20 mmol) was slowly added and refluxed for 4-5 hr. The reaction mixture was cooled to room temperature, poured into ice-cold water and neutralized with dil. HCl. The separated solid product was filtered, washed with water and dried at room temperature to get an analytically pure compound (**3a-t**), as a light brown solid.

- **General process for the synthesis of thiazolo[3,2-*a*]pyrimidine (4a-t)**

A mixture of **3a-t** (10 mmol) and 2-bis(methylthio)methylene malononitrile (10 mmol) in 10 mL of DMF and anhydrous potassium carbonate (10 mmol) was heated to reflux for 30 min. After the completion of the reaction, the reaction mixture was cooled to room temperature, poured into ice-cold water and neutralized with dil. HCl. The

separated solid was filtered, washed with water and purified by recrystallization from DMF to afford crystals **(4a-t)**.

6-cyano-5-imino-*N*-(4-methoxyphenyl)-3-methyl-7-(methylthio)-5*H*-thiazolo[3,2-*a*]pyrimidine-2-carboxamide (CNTHNH-1)

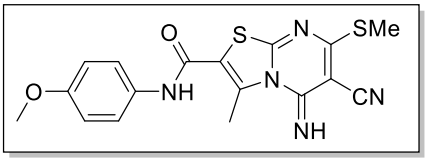

Red crystals, Yield: 88%, mp 213-215°C with decomposition; FTIR (ATR, ν_{max}, cm^{-1}): 3281, 2204, 1631; ^{1}H NMR (400 MHz, DMSO-d_6) δ 10.49 (s, 1H), 9.76 (s, 1H), 7.57 (d, J = 8.6 Hz, 2H), 6.96 (d, J = 8.7 Hz, 2H), 3.76 (s, 3H), 2.94 (s, 3H), 2.56 (s, 3H); MS (*m*/*z*): 385 (M^+); Anal. Calcd. For $C_{17}H_{15}N_5O_2S_2$: C, 52.97; H, 3.92; N, 18.17; Found: C, 52.99; H, 3.95; N, 18.19.

6-cyano-5-imino-3-methyl-7-(methylthio)-*N*-(*p*-tolyl)-5*H*-thiazolo[3,2-*a*]pyrimidine-2-carboxamide (CNTHNH-2)

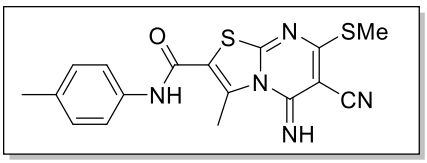

Yellow Crystals, Yield: 95%, mp 226-228°C; FTIR (ATR, ν_{max}, cm^{-1}): 3289, 2202, 1638 ; ^{1}H NMR (400 MHz, DMSO-d_6) δ 10.55 (s, 1H), 9.81 (s, 1H), 7.54 (d, J = 8.1 Hz, 2H), 7.19 (d, J = 8.1 Hz, 2H), 2.93 (s, 3H), 2.56 (s, 3H), 2.30 (s, 3H); ^{13}C NMR (100 MHz, DMSO) δ 167.91, 165.63, 158.42, 139.66, 135.93, 134.26, 129.70, 129.49, 121.23, 120.97, 118.22, 115.78, 85.71, 21.00, 19.04, 13.19; MS (*m*/*z*): 369 (M^+); Anal. Calcd. For $C_{17}H_{15}N_5OS_2$: C, 55.27; H, 4.09; N, 18.96; Found: C, 55.25; H, 4.10; N, 18.93.

6-cyano-5-imino-3-methyl-7-(methylthio)-*N*-phenyl-5*H*-thiazolo[3,2-*a*]pyrimidine-2-carboxamide (CNTHNH-3)

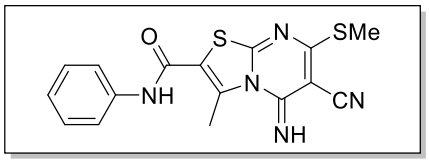

Yellow Crystals, Yield: 91%, mp 201-203°C; FTIR (ATR, ν_{max}, cm^{-1}): 3284, 2208, 1665; ^{1}H NMR (400 MHz, DMSO-d_6) δ 10.64 (s, 1H), 7.70 – 7.55 (m, 3H), 7.39 (t, J = 7.8 Hz, 2H), 7.17 (t, J = 7.4 Hz, 1H), 2.94 (s, 3H), 2.57 (s, 3H); ^{13}C NMR (100 MHz, DMSO) δ 167.96, 165.64, 158.65, 153.46, 139.79, 138.43, 132.17, 129.33, 125.15, 122.87, 120.96, 118.15, 115.76, 85.72, 19.03, 13.19; MS (*m*/*z*): 355 (M^+); Anal. Calcd. For $C_{16}H_{13}N_5OS_2$: C, 54.07; H, 3.69; N, 19.70; Found: C, 54.13; H, 3.72; N, 19.74.

_N_-(3-chlorophenyl)-6-cyano-5-imino-3-methyl-7-(methylthio)-5_H_-thiazolo[3,2-_a_]pyrimidine-2-carboxamide (CNTHNH-4)

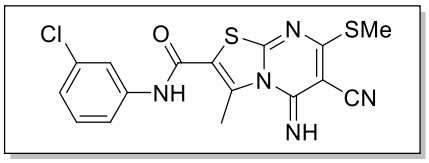

Yellow Crystals, Yield: 93%, mp 216-218°C; FTIR (ATR, ν_{max}, cm^{-1}): 3202, 2210, 1677 ; ^{1}H NMR (400 MHz, DMSO-d_6) δ 10.80 (s, 1H), 9.81 (s, 1H), 7.83 (t, J = 2.0 Hz, 1H), 7.59 (dd, J = 8.1, 2.1 Hz, 2H), 7.42 (t, J = 8.1 Hz, 2H), 7.24 (dd, J = 8.1, 2.1 Hz, 2H), 2.94 (s, 3H), 2.57 (s, 3H); ^{13}C NMR (100 MHz, DMSO) δ 167.52, 165.08, 158.40, 152.93, 139.80, 139.42, 133.06, 130.52, 124.30, 119.93, 118.82, 117.28, 115.18, 85.27, 18.56, 12.72; MS (*m*/*z*): 389 (M^+); Anal. Calcd. For $C_{16}H_{12}ClN_5OS_2$: C, 49.29; H, 3.10; N, 17.96; Found: C, 49.32; H, 3.14; N, 17.97.

6-cyano-_N_-(2,4-dimethylphenyl)-5-imino-3-methyl-7-(methylthio)-5_H_-thiazolo[3,2-_a_]pyrimidine-2-carboxamide (CNTHNH-5)

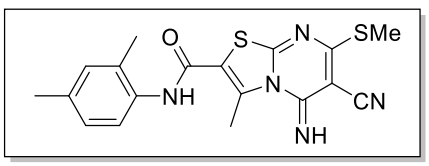

Yellow Crystals, Yield: 90%, mp 242-244°C; FTIR (ATR, ν_{max}, cm^{-1}): 2210, 1679; ^{1}H NMR (400 MHz, DMSO-d_6) δ 10.06 (s, 1H), 9.41 (s, 1H), 7.23 (d, J = 8.0 Hz, 2H), 7.11 (s, 1H), 7.05 (d, J = 7.9 Hz, 2H), 3.00 (s, 3H), 2.56 (s, 3H), 2.29 (s, 3H), 2.20 (s,

3H); ^{13}C NMR (100 MHz, DMSO-d_6) δ 167.38, 165.07, 158.42, 152.99, 139.66, 135.85, 133.17, 132.65, 131.02, 126.70, 126.09, 115.29, 85.23, 20.52, 18.51, 17.88, 12.68; MS (*m*/*z*): 383 (M^+); Anal. Calcd. For $C_{18}H_{17}N_5OS_2$: C, 56.38; H, 4.47; N, 18.26; Found: C, 56.40; H, 4.52; N, 18.29.

_N_-(4-chlorophenyl)-6-cyano-5-imino-3-methyl-7-(methylthio)-5_H_-thiazolo[3,2-_a_]pyrimidine-2-carboxamide (CNTHNH-6)

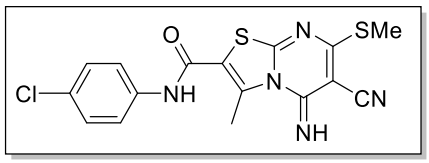

Yellow Crystals, Yield: 89%, mp 230-232°C; FTIR (ATR, ν_{max}, cm^{-1}): 3268, 2202, 1639; ^{1}H NMR (400 MHz, DMSO-d_6) δ 10.75 (s, 1H), 9.96 (s, 1H), 7.69 (d, J = 8.9 Hz, 2H), 7.45 (d, J = 8.9 Hz, 2H), 2.93 (s, 3H), 2.56 (s, 3H); MS (*m*/*z*): 389 (M^+); Anal. Calcd. For $C_{16}H_{12}ClN_5OS_2$: C, 49.29; H, 3.10; N, 17.96; Found: C, 49.24; H, 3.06; N, 17.92.

6-cyano-_N_-(2,6-dimethylphenyl)-5-imino-3-methyl-7-(methylthio)-5_H_-thiazolo[3,2-_a_]pyrimidine-2-carboxamide (CNTHNH-7)

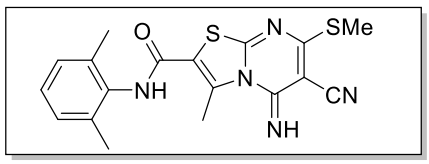

Yellow Crystals, Yield: 92%, mp 238-240°C; FTIR (ATR, ν_{max}, cm^{-1}): 3218, 2201, 1630; ^{1}H NMR (400 MHz, DMSO-d_6) δ 9.94 (s, 1H), 9.31 (s, 1H), 7.16 (s, 3H), 3.04 (s, 3H), 2.56 (s, 3H), 2.21 (s, 3H); MS (*m*/*z*): 383 (M^+); Anal. Calcd. For $C_{18}H_{17}N_5OS_2$: C, 56.38; H, 4.47; N, 18.26; Found: C, 56.36; H, 4.43; N, 18.24.

6-cyano-_N_-(4-fluorophenyl)-5-imino-3-methyl-7-(methylthio)-5_H_-thiazolo[3,2-_a_]pyrimidine-2-carboxamide (CNTHNH-8)

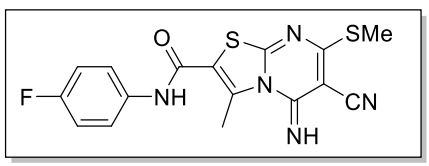

Yellow Crystals, Yield: 90%, mp 237-239°C; FTIR (ATR, ν_{max}, cm^{-1}): 3310, 2208, 1620; ^{1}H NMR (400 MHz, DMSO-d_6) δ 10.67 (s, 1H), 9.93 (s, 1H), 7.68 (dd, J = 9.1, 5.0 Hz, 2H), 7.24 (t, J = 8.9 Hz, 2H), 2.94 (s, 3H), 2.56 (s, 3H); MS (m/z): 373 (M^+); Anal. Calcd. For $C_{16}H_{12}FN_5OS_2$: C, 51.46; H, 3.24; N, 18.75; Found: C, 51.50; H, 3.22; N, 18.76.

_N_-(4-bromophenyl)-6-cyano-5-imino-3-methyl-7-(methylthio)-5_H_-thiazolo[3,2-_a_]pyrimidine-2-carboxamide (CNTHNH-9)

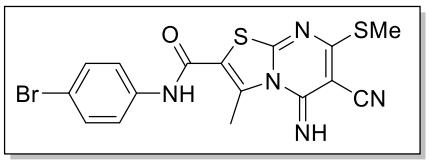

Yellow Crystals, Yield: 95%, mp 248-250°C; FTIR (ATR, ν_{max}, cm^{-1}): 3309, 2207, 1680; ^{1}H NMR (400 MHz, DMSO-d_6) δ 10.75 (s, 1H), 10.00 (s, 1H), 7.64 (d, J = 8.9 Hz, 2H), 7.58 (d, J = 8.9 Hz, 2H), 2.93 (s, 3H), 2.56 (s, 3H); MS (m/z): 434 (M^+); Anal. Calcd. For $C_{16}H_{12}BrN_5OS_2$: C, 44.25; H, 2.78; N, 16.12; Found: C, 44.27; H, 2.79; N, 16.15.

6-cyano-5-imino-_N_-(2-methoxyphenyl)-3-methyl-7-(methylthio)-5_H_-thiazolo[3,2-_a_]pyrimidine-2-carboxamide (CNTHNH-10)

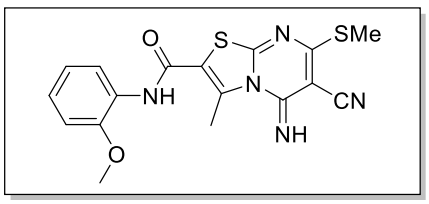

Yellow Crystals, Yield: 94%, mp 212-214°C; FTIR (ATR, ν_{max}, cm^{-1}): 3291, 2201, 1619; ^{1}H NMR (400 MHz, DMSO-d_6) δ 9.80 (s, 1H), 9.03 (s, 1H), 7.68 (d, J = 7.8 Hz, 1H), 7.24 (td, J = 7.8, 1.7 Hz, 1H), 7.12 (dd, J = 8.3, 1.4 Hz, 1H), 6.99 (td, J = 7.7, 1.4 Hz, 1H), 3.84 (s, 3H), 3.00 (s, 3H), 2.56 (s, 3H); MS (m/z): 385 (M^+); Anal. Calcd. For $C_{17}H_{15}N_5O2S_2$: C, 52.97; H, 3.92; N, 18.17; Found: C, 52.95; H, 3.89; N, 18.14.

6-cyano-5-imino-3-methyl-7-(methylthio)-_N_-(3-(trifluoromethyl)phenyl)-5_H_-thiazolo[3,2-_a_]pyrimidine-2-carboxamide (CNTHNH-11)

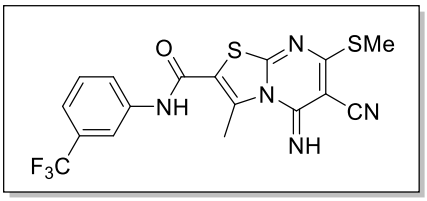

Yellow Crystals, Yield: 62%, mp 240-242°C; MS (*m*/*z*): 423 (M^+); Anal. Calcd. For $C_{17}H_{12}F_3N_5OS_2$: C, 48.22; H, 2.86; N, 16.54; Found: C, 48.16; H, 2.77; N, 16.42.

6-cyano-5-imino-*N*-(3-methoxyphenyl)-3-methyl-7-(methylthio)-5*H*-thiazolo[3,2-*a*]pyrimidine-2-carboxamide (CNTHNH-12)

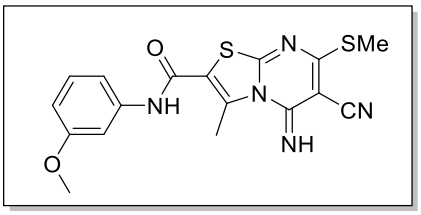

Yellow Crystals, Yield: 78%, mp 207-209°C; MS (*m*/*z*): 385 (M^+); Anal. Calcd. For $C_{17}H_{15}N_5O_2S_2$: C, 52.97; H, 3.92; N, 18.17; Found: C, 52.99; H, 3.91; N, 18.24.

6-cyano-*N*-(2-fluorophenyl)-5-imino-3-methyl-7-(methylthio)-5*H*-thiazolo[3,2-*a*]pyrimidine-2-carboxamide (CNTHNH-13)

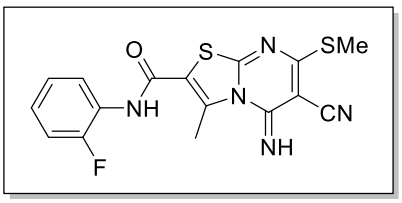

Yellow Crystals, Yield: 71%, mp 233-234°C; MS (*m*/*z*): 473 (M^+); Anal. Calcd. For $C_{16}H_{12}FN_5OS_2$: C, 51.46; H, 3.24; N, 18.75; Found: C, 51.62; H, 3.39; N, 18.83.

***N*-(3-chloro-4-fluorophenyl)-6-cyano-5-imino-3-methyl-7-(methylthio)-5*H*-thiazolo[3,2-*a*]pyrimidine-2-carboxamide (CNTHNH-14)**

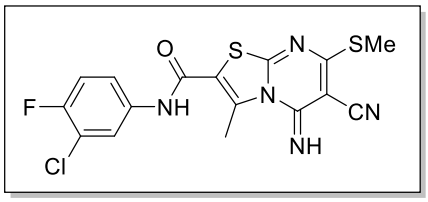

Yellow Crystals, Yield: 75%, mp 239-241°C; MS (*m*/*z*): 407 (M^+); Anal. Calcd. For $C_{16}H_{11}ClFN_5OS_2$: C, 47.12; H, 2.72; N, 17.17; Found: C, 47.03; H, 2.73; N, 17.20.

6-cyano-*N*-(3,4-dimethylphenyl)-5-imino-3-methyl-7-(methylthio)-5*H*-thiazolo[3,2-*a*]pyrimidine-2-carboxamide (CNTHNH-15)

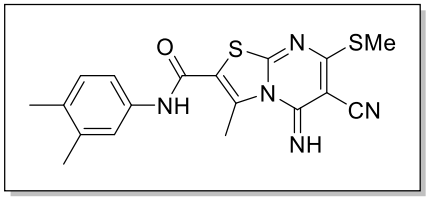

Yellow Crystals, Yield: 82%, mp 247-249°C; MS (*m*/*z*): 383 (M^+); Anal. Calcd. For $C_{18}H_{17}N_5OS_2$: C, 56.38; H, 4.47; N, 18.26; Found: C, 56.29; H, 4.46; N, 18.25.

***N*-(2-bromo-4-chlorophenyl)-6-cyano-5-imino-3-methyl-7-(methylthio)-5*H*-thiazolo[3,2-*a*]pyrimidine-2-carboxamide (CNTHNH-16)**

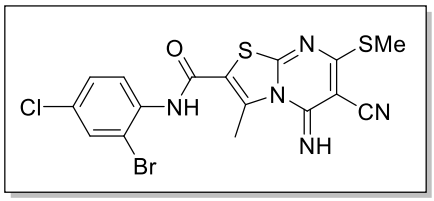

Yellow Crystals, Yield: 85%, mp 221-223°C; MS (*m*/*z*): 424 (M^+); Anal. Calcd. For $C_{16}H_{11}Cl_2N_5OS_2$: C, 41.00; H, 2.37; N, 14.94; Found: C, 41.01; H, 2.32; N, 14.77.

6-cyano-*N*-(3,4-dichlorophenyl)-5-imino-3-methyl-7-(methylthio)-5*H*-thiazolo[3,2-*a*]pyrimidine-2-carboxamide (CNTHNH-17)

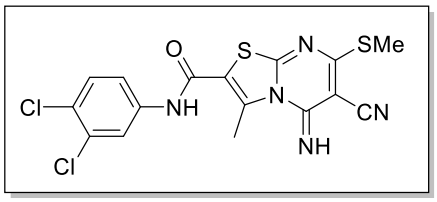

Yellow Crystals, Yield: 80%, mp 227-229°C; MS (*m*/*z*): 424 (M^+); Anal. Calcd. For $C_{16}H_{11}Cl_2N_5OS_2$: C, 45.29; H, 2.61; N, 16.51; Found: C, 45.18; H, 2.55; N, 16.49.

6-cyano-*N*-(3-fluorophenyl)-5-imino-3-methyl-7-(methylthio)-5*H*-thiazolo[3,2-*a*]pyrimidine-2-carboxamide (CNTHNH-18)

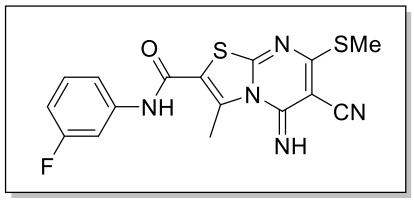

Yellow Crystals, Yield: 63%, mp 232-234°C; MS (*m*/*z*): 373 (M^+); Anal. Calcd. For $C_{16}H_{12}FN_5OS_2$: C, 51.46; H, 3.24; N, 18.75; Found: C, 51.61; H, 3.55; N, 18.79.

***N*-(3-bromophenyl)-6-cyano-5-imino-3-methyl-7-(methylthio)-5*H*-thiazolo[3,2-*a*]pyrimidine-2-carboxamide (CNTHNH-19)**

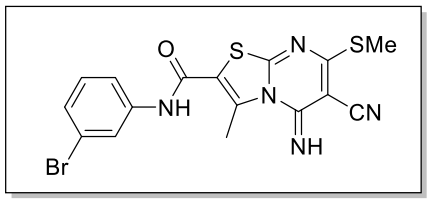

Yellow Crystals, Yield: 87%, mp 244-246°C; MS (*m*/*z*): 434 (M^+); Anal. Calcd. For $C_{16}H_{12}BrN_5OS_2$: C, 44.25; H, 2.78; N, 16.12; Found: C, 44.22; H, 2.71; N, 16.06.

6-cyano-5-imino-3-methyl-7-(methylthio)-*N*-(m-tolyl)-5*H*-thiazolo[3,2-*a*]pyrimidine-2-carboxamide (CNTHNH-20)

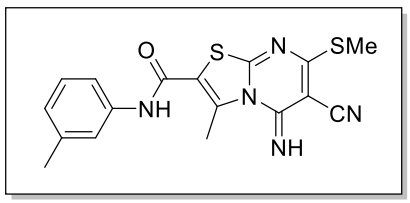

Yellow Crystals, Yield: 82%, mp 220-222°C; MS (*m*/*z*): 369 (M^+); Anal. Calcd. For $C_{17}H_{15}N_5OS_2$: C, 55.27; H, 4.09; N, 18.96; Found: C, 55.28; H, 4.18; N, 19.03.

2.5.1 Experimental protocol of molecular docking study

The ChemSketch 2021.2.0 software was used for the generation of ligand structures. Furthermore, the energy minimization of every molecule was performed using the Dundee PRODRG2 server and Autodock Vina 1.1.2 was used to for the docking studies. Topoisomerase II alpha was downloaded from PDB database (1ZXM). Heteroatoms were excluded to make the structure receptor free from all ligands prior to docking. The protein preparation was done by addition of kollaman charge, solvation parameters and polar hydrogens. The grid box size was set to 40, 40 and 40 Å for x, y and z correspondingly. The grid center was set to 49.588, 3.725 and 22.091 for x, y and z individually. The spacing among grid points was 0.375 angstroms and the exhaustiveness was equal to 40. Powerful molecular graphics viewer Discovery Studio Visualizer v21.0 was used to figure out the most probable binding mode.

2.5.2 Cytotoxic evaluation

2.5.2.1 Materials and methods

Fetal bovine serum (FBS), Dulbecco's modified eagle medium (DMEM) and MTT [3-(4,5-dimethylthiazol-2-yl)-2,5-diphenyltetrazolium bromide] were purchased from Sigma-Aldrich Chemicals. 96 well cell culture plates were purchased from Thermo Fisher Scientific. Human lung adenocarcinoma cell line (A549), human breast carcinoma cell line (MCF-7) and human cervical cancer cell line (HeLa) were obtained from the American Type Culture Collection (ATCC), India.

2.5.2.2 Cell culture

Cell lines were cultured in DMEM medium containing 10% fetal bovine serum, 10 ml/l antibiotic-antimycotic solution (10,000 Units/ml penicillin, 10 mg/l streptomycin and 25 µg/ml amphotericin B) and this culture was kept in CO_2 incubator with 90% humidified atmosphere and 5% CO_2 at 37°C.

2.5.2.3 Preparation of samples for MTT assay

DMSO (dimethyl sulfoxide) was used to dissolve the test compounds **4a-j** with a stock concentration of 10 µM. Subsequently, with sterile PBS (1X) dilutions were made to achieve. The dilutions were made with sterile PBS (1X) to get the chosen concentrations. This was followed by filtration with a 0.22 µm sterile filter and

subjected to exposure to UV light for 20 minutes. Then, each sample was added to a 96 well microtiter plate containing cells.

2.6 MTT assay

MTT assay is used to determine the cell viability, thereby analyzing the cytotoxicity of the synthesized molecules. Here, the protocol followed is referenced by Sekhar. The exponentially dividing cell concentration of $5x10^3$ was seeded into the microtiter plate (counted by trypan blue exclusion dye method). Furthermore, cells were grown till 60-70% confluence after which compounds **4a-j** with the final concentration ranging from 0.1, 1, 5 and 10 µM were added to the culture medium and as a positive control doxorubicin was utilized and no compound was added to the negative control and incubation for 24 and 48 hours at 37°C with 5% CO_2 and 90% humidified atmosphere in a CO_2 incubator was performed. Soon after, the media of the wells were replaced with 90µl of fresh serum-free media and 10 µl of MTT (5 mg/mL of PBS) and again incubated at 37°C for 2 hr, whereas the above media was disposed and the plate was dried for 30 minutes. Then into each well, 100 µL of DMSO was added at 37°C and continued for 5 minutes. The purple formazan crystals were dissolved and were instantly measured on Spectra Max plus 384 UV-Visible plate reader at 570 nm. Using the absorbance values relative to the control was used to determine IC_{50} values (**Table 3**).

2.7 Spectral Data

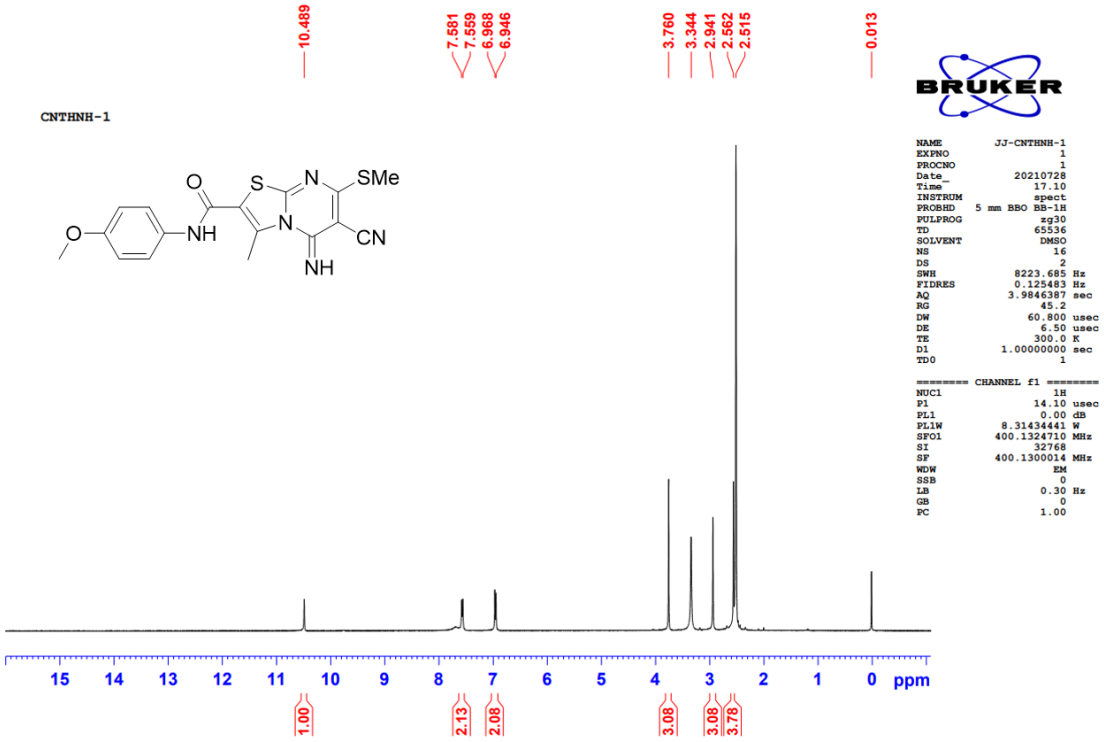

Fig. 1: Representative ^{1}H NMR spectrum of compound CNTHNH-1

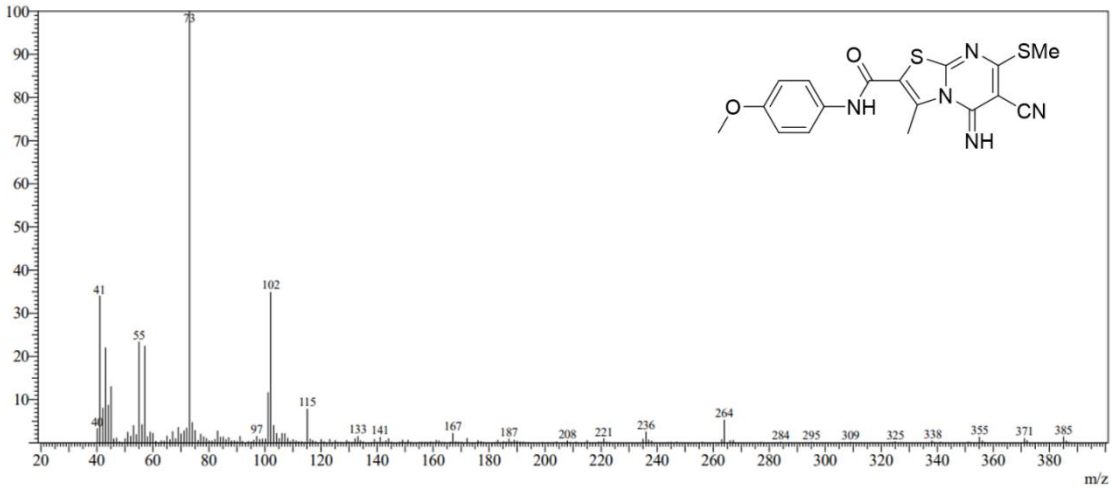

Fig. 2: Representative mass spectrum of compound CNTHNH-1

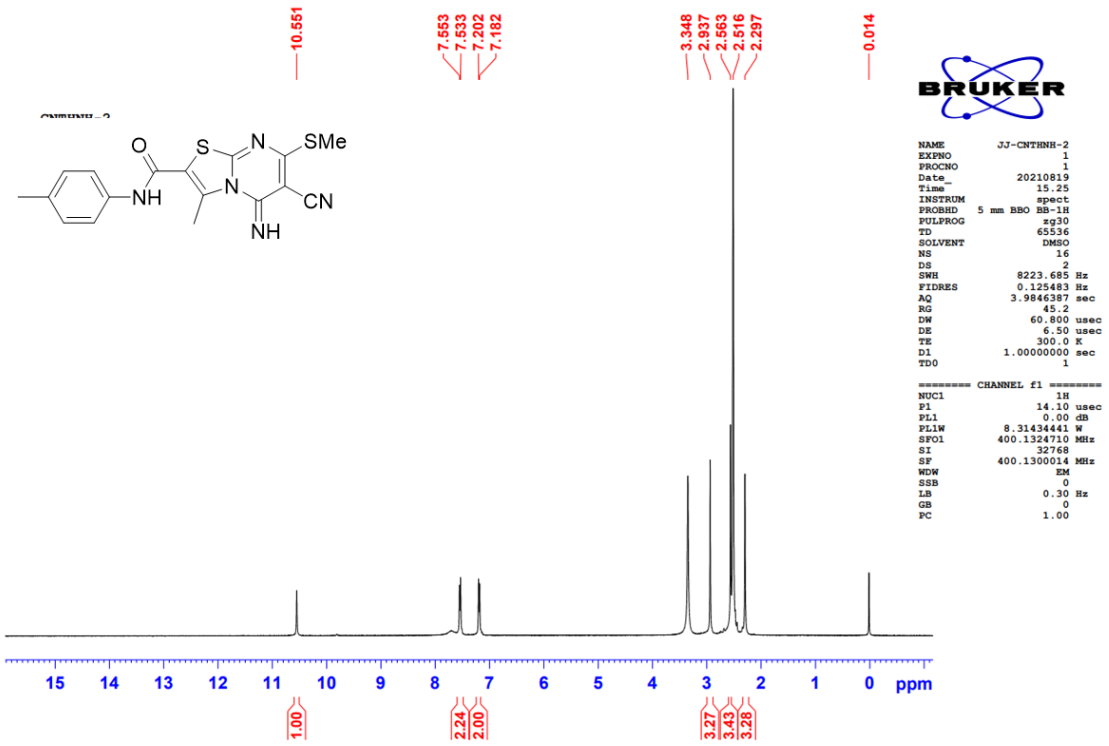

Fig. 3: Representative ^{1}H NMR spectrum of compound CNTHNH-2

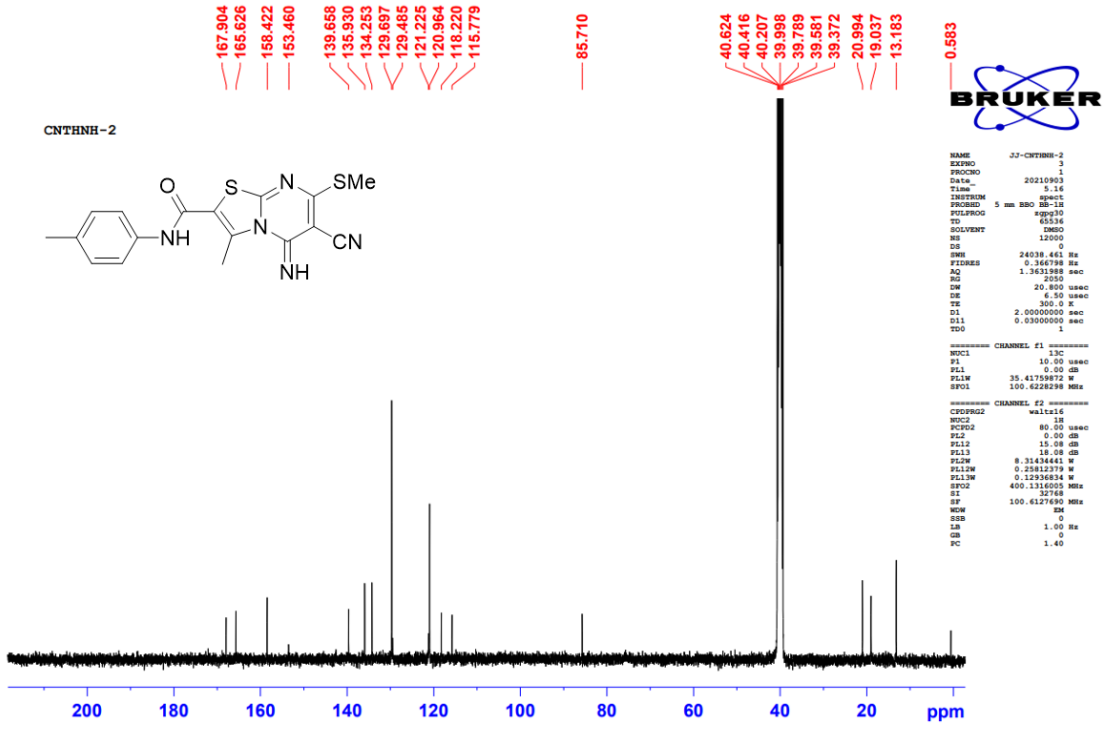

Fig. 4: Representative ^{13}C NMR spectrum of compound CNTHNH-2

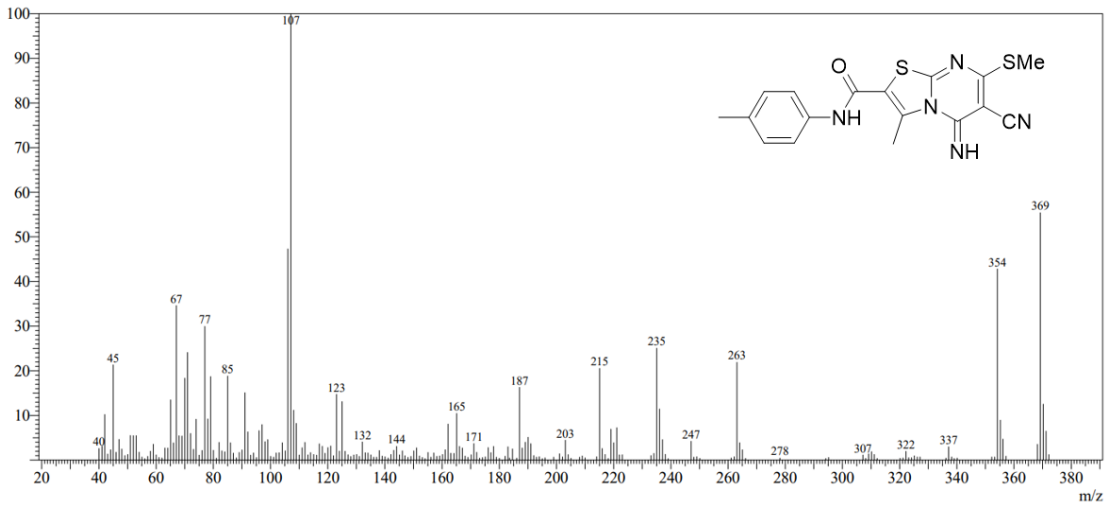

Fig. 5: Representative mass spectrum of compound CNTHNH-2

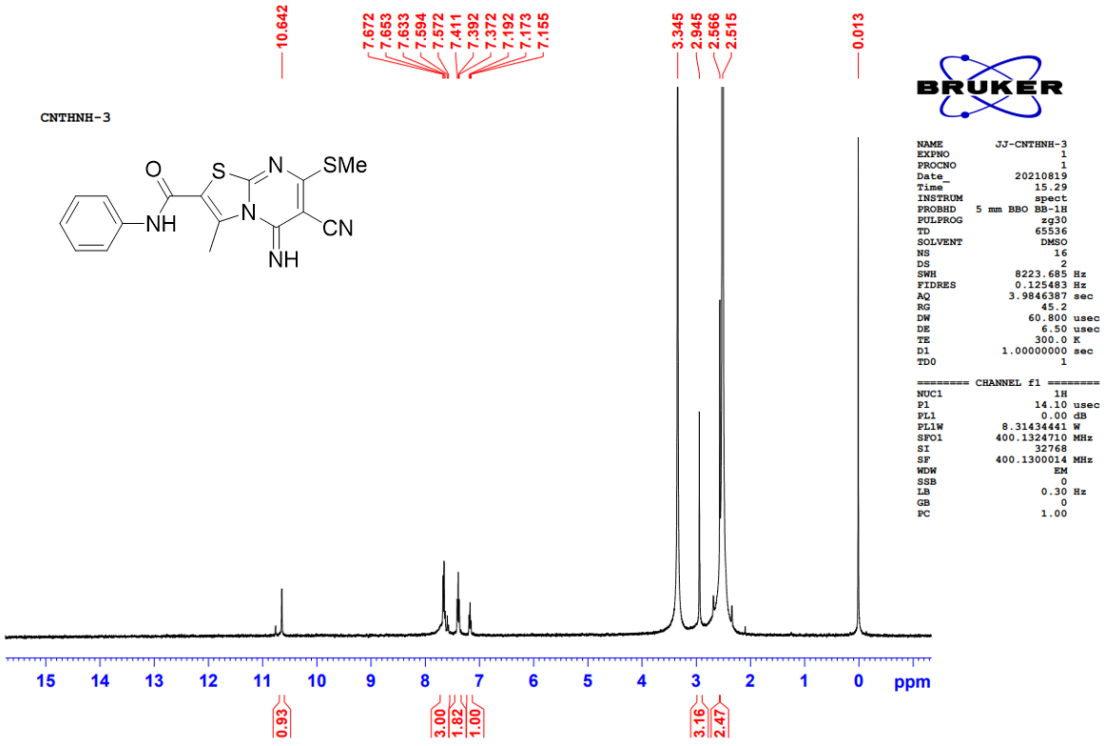

Fig. 6: Representative ^{1}H NMR spectrum of compound CNTHNH-3

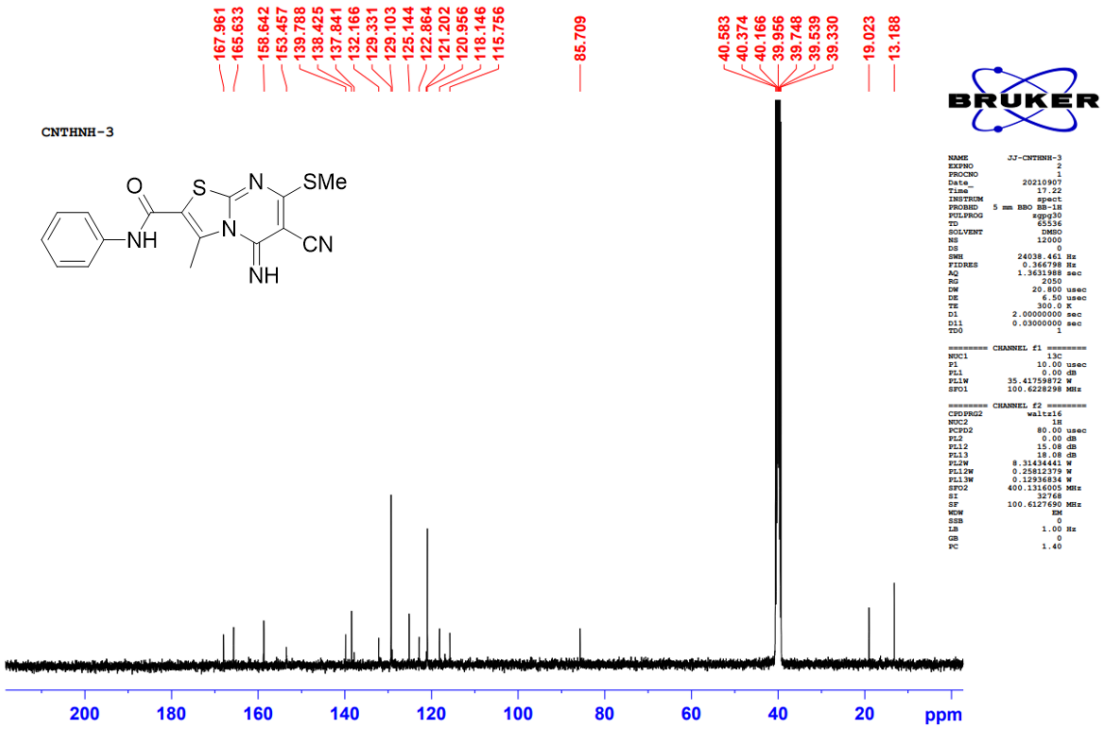

Fig. 7: Representative ^{13}C NMR spectrum of compound CNTHNH-3

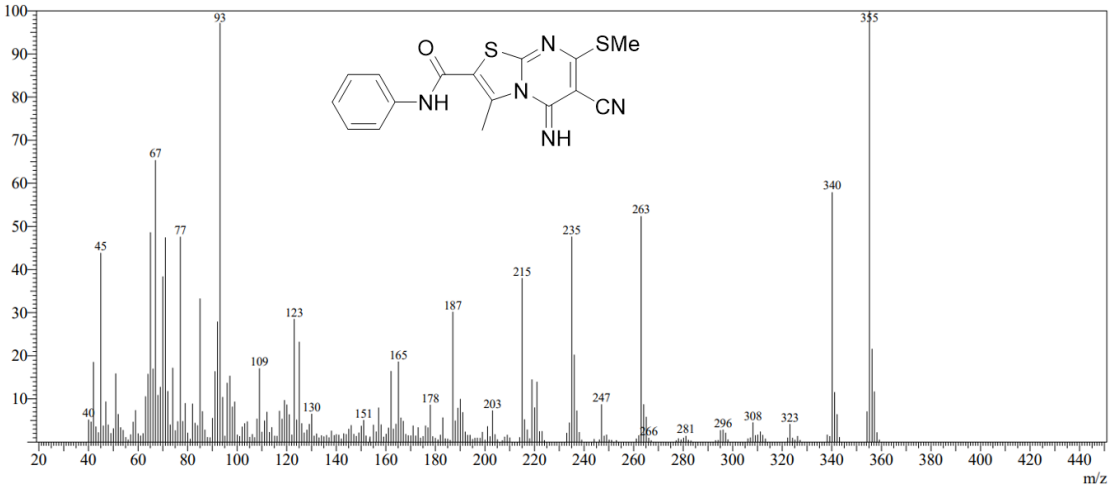

Fig. 8: Representative mass spectrum of compound CNTHNH-3

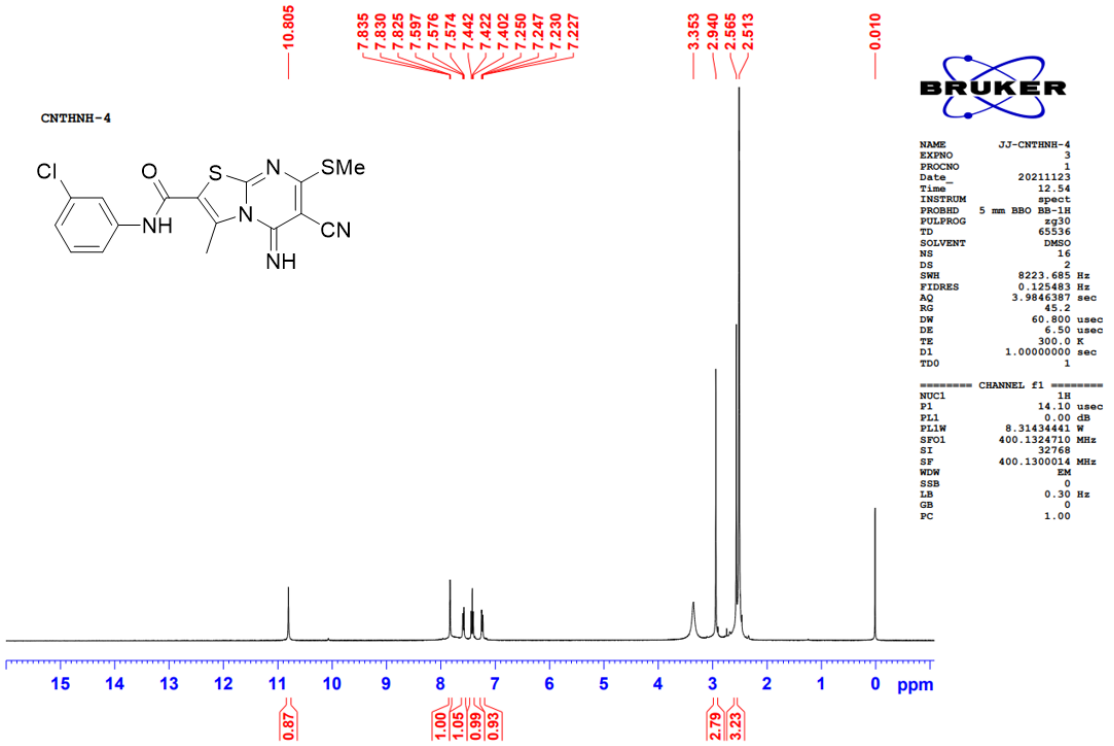

Fig. 9: Representative ^{1}H NMR spectrum of compound CNTHNH-4

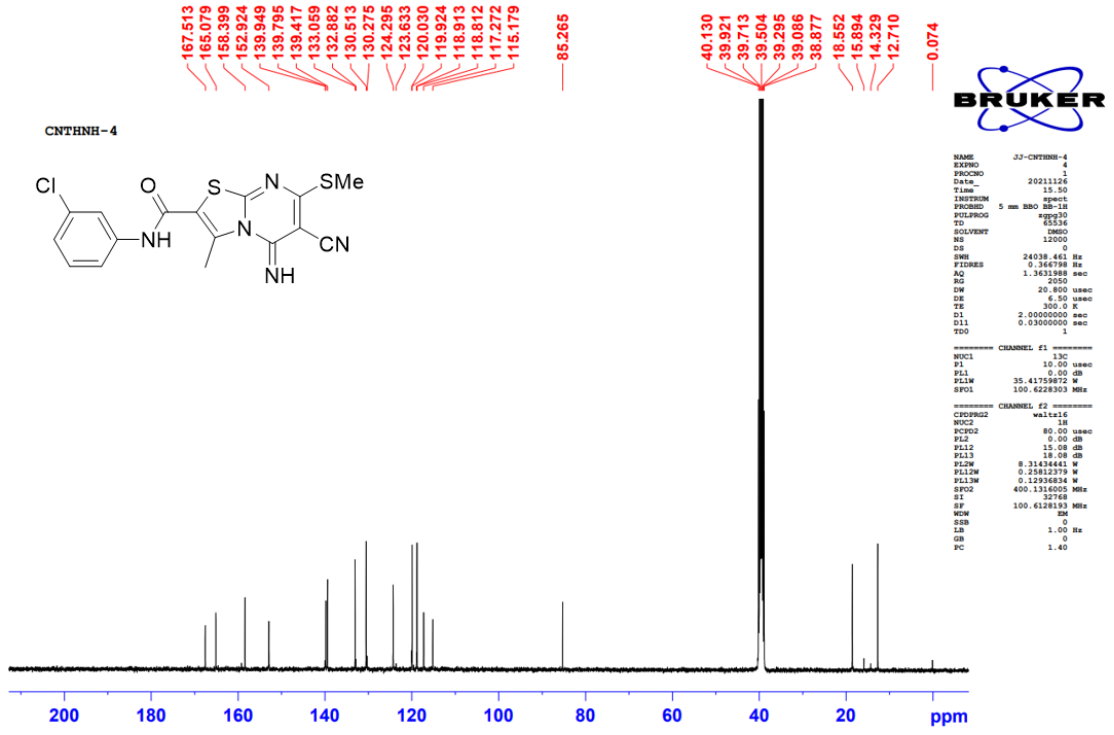

Fig. 10: Representative ^{13}C NMR spectrum of compound CNTHNH-4

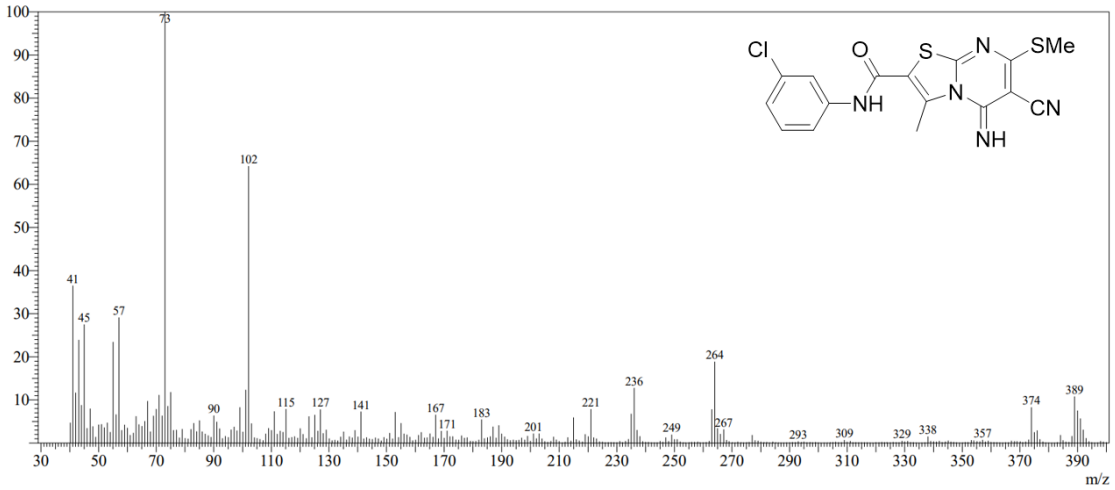

Fig. 11: Representative mass spectrum of compound CNTHNH-4

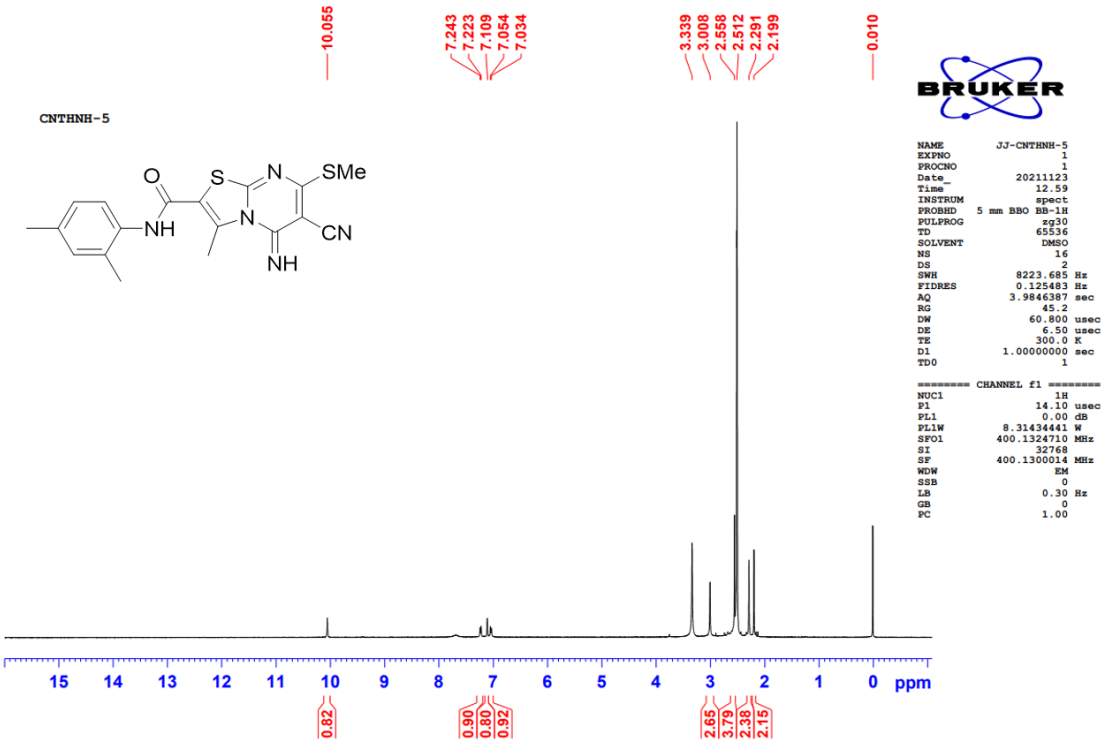

Fig. 12: Representative ^{1}H NMR spectrum of compound CNTHNH-5

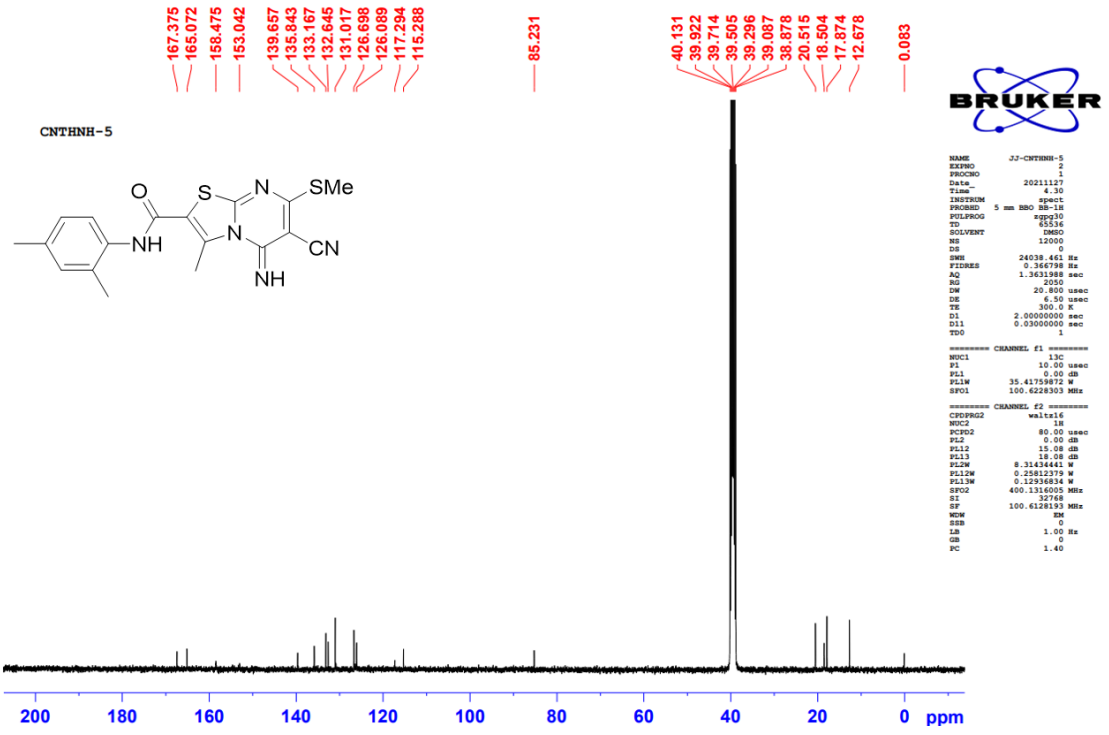

Fig. 13: Representative ^{13}C NMR spectrum of compound CNTHNH-5

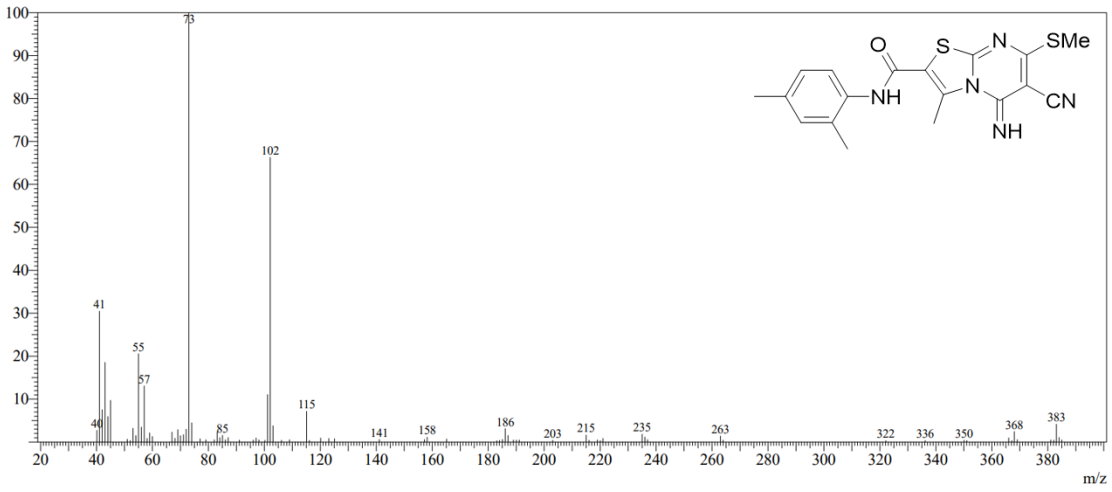

Fig. 14: Representative mass spectrum of compound CNTHNH-5

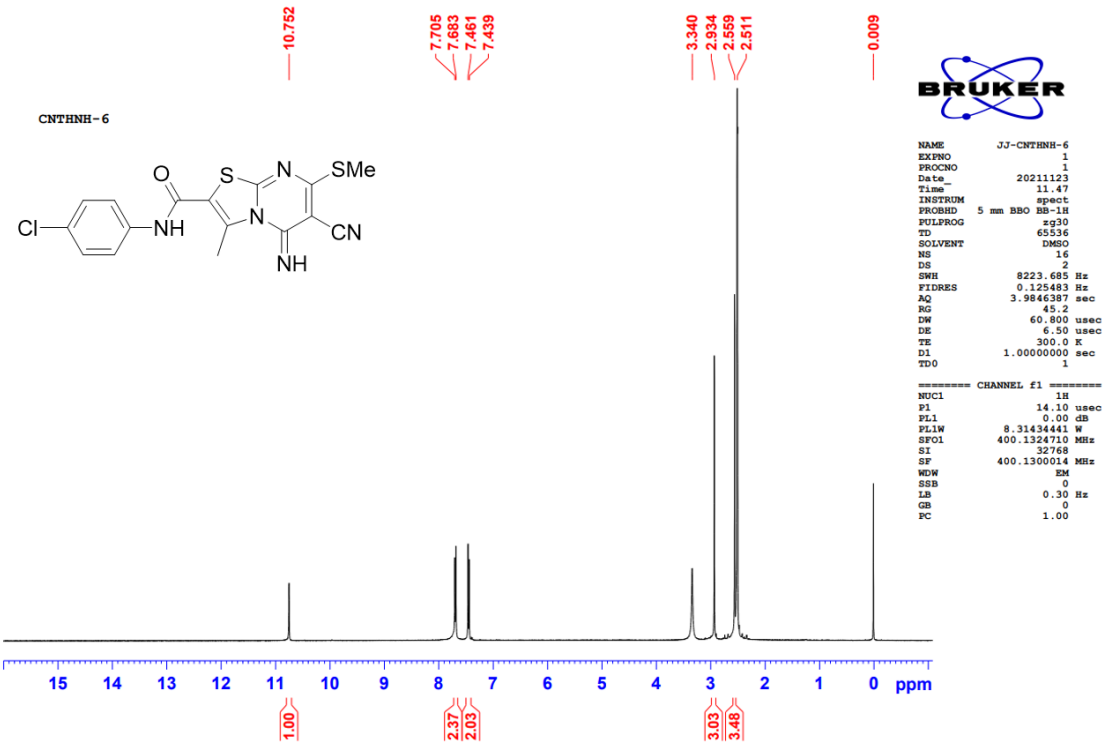

Fig. 15: Representative ^{1}H NMR spectrum of compound CNTHNH-6

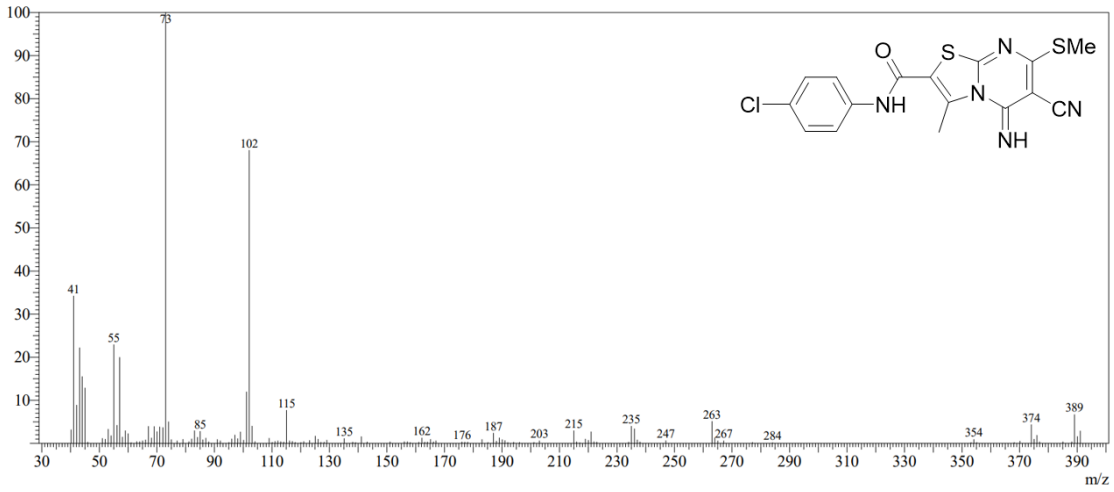

Fig. 16: Representative mass spectrum of compound CNTHNH-6

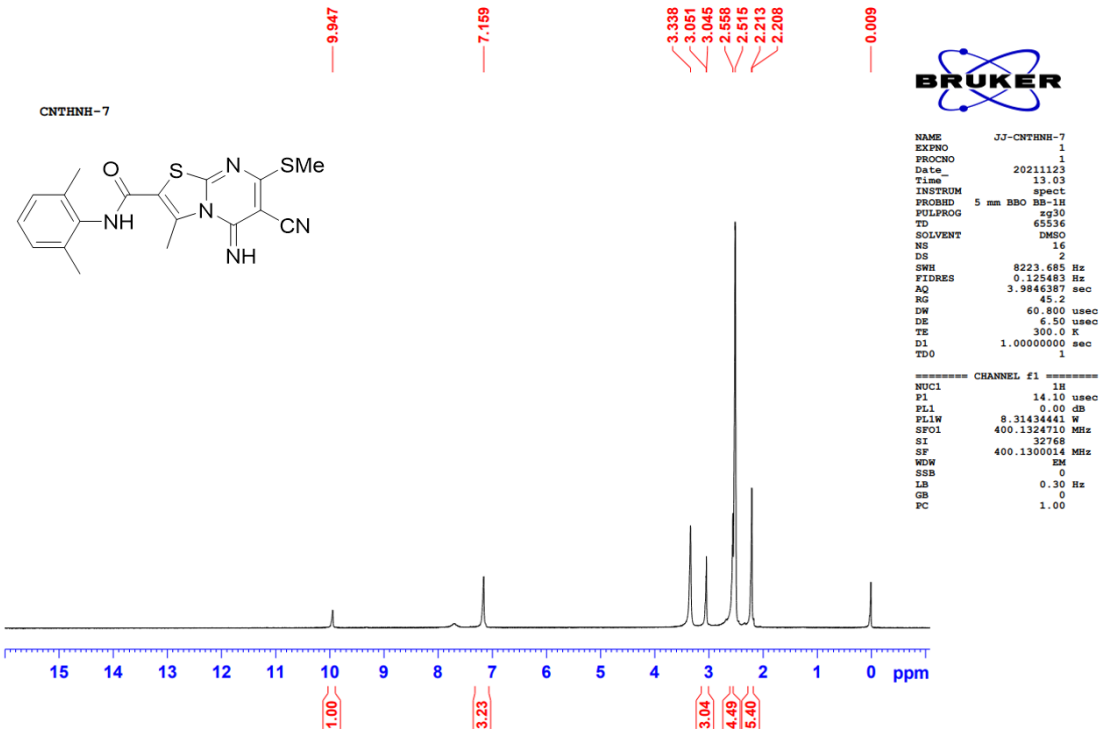

Fig. 17: Representative ^{1}H NMR spectrum of compound CNTHNH-7

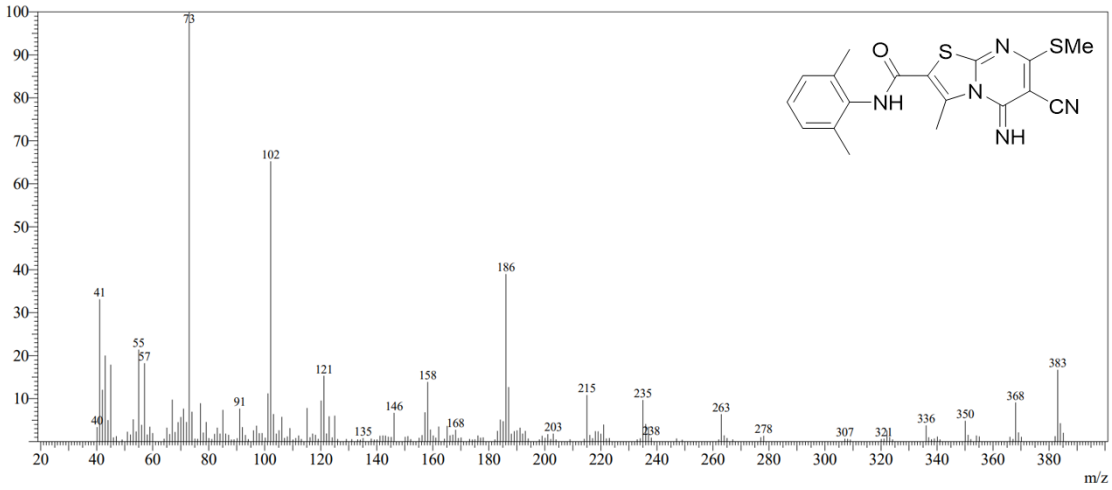

Fig. 18: Representative mass spectrum of compound CNTHNH-7

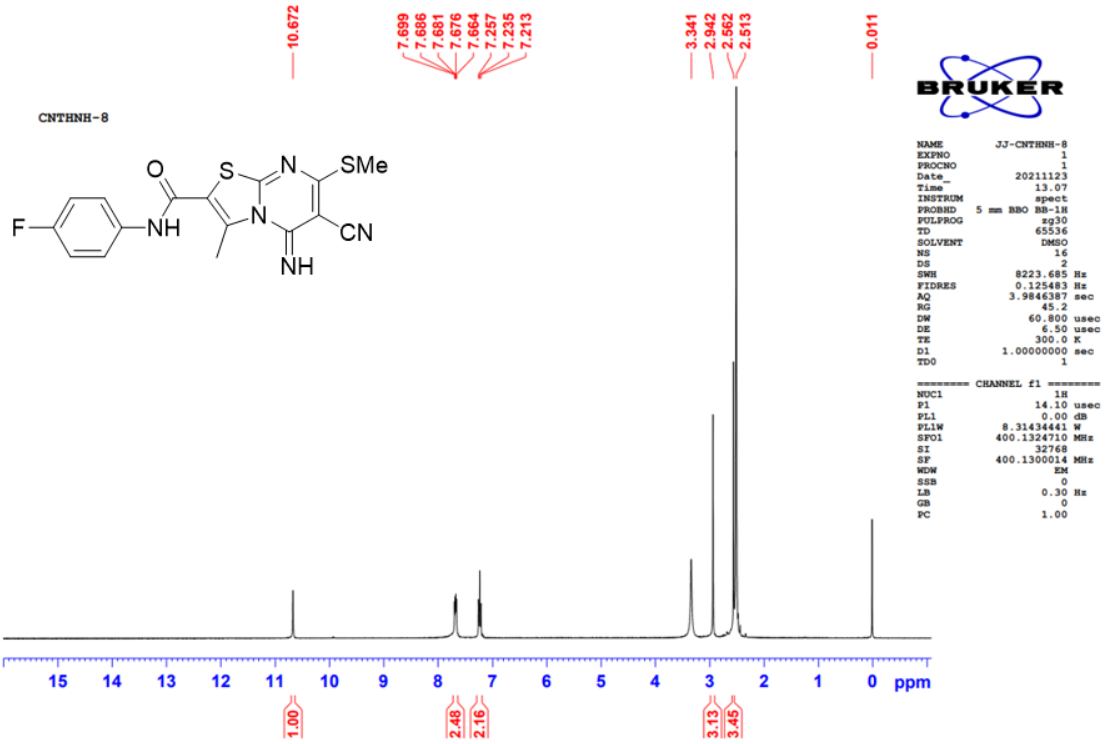

Fig. 19: Representative ^{1}H NMR spectrum of compound CNTHNH-8

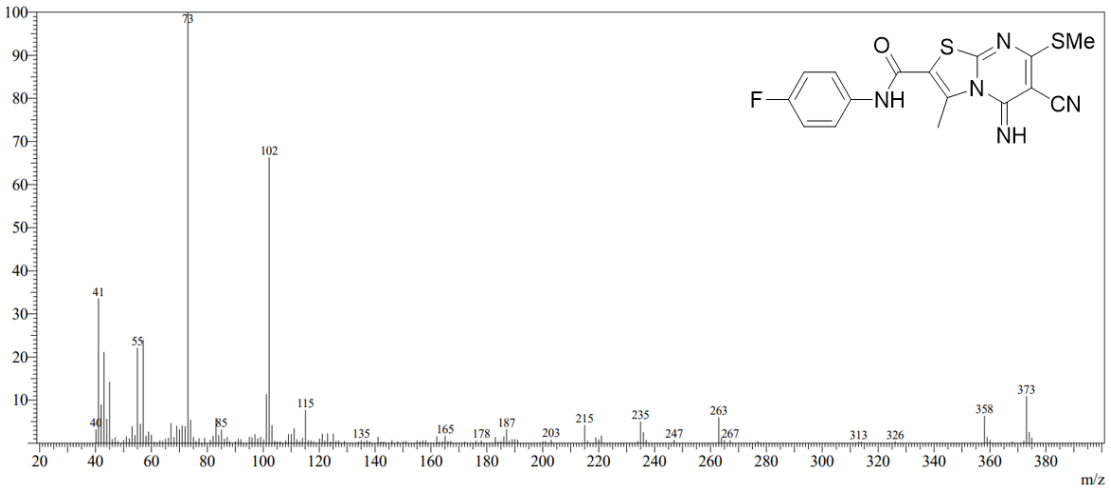

Fig. 20: Representative mass spectrum of compound CNTHNH-8

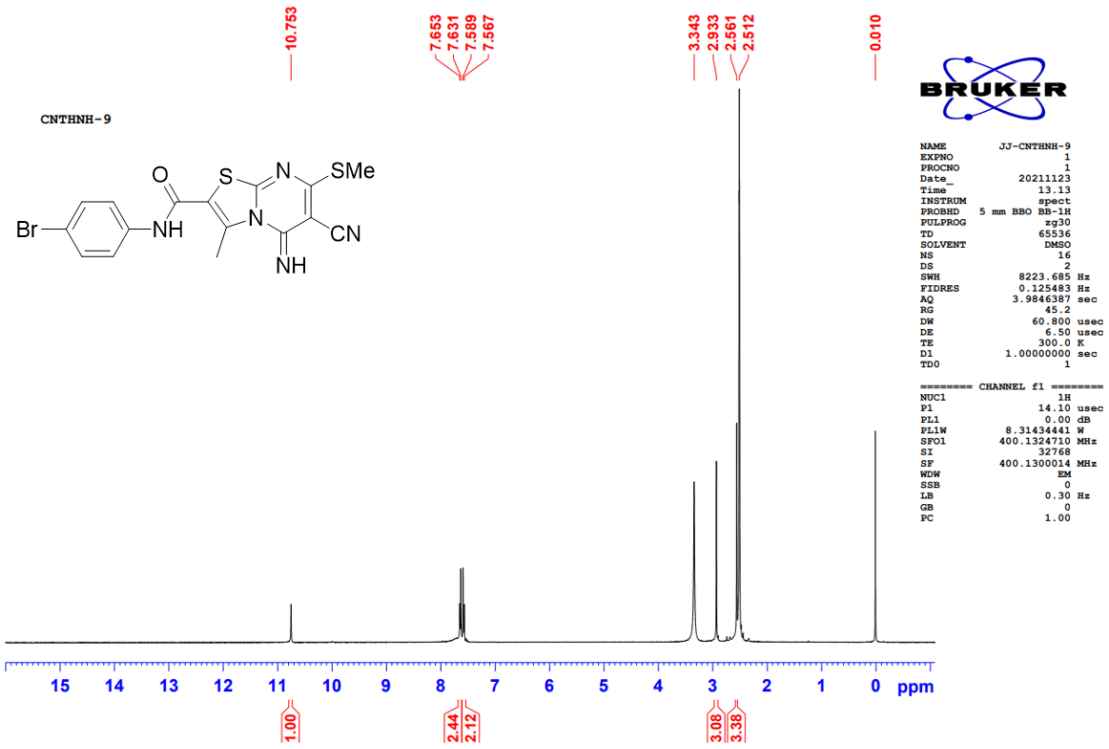

Fig. 21: Representative ^{1}H NMR spectrum of compound CNTHNH-9

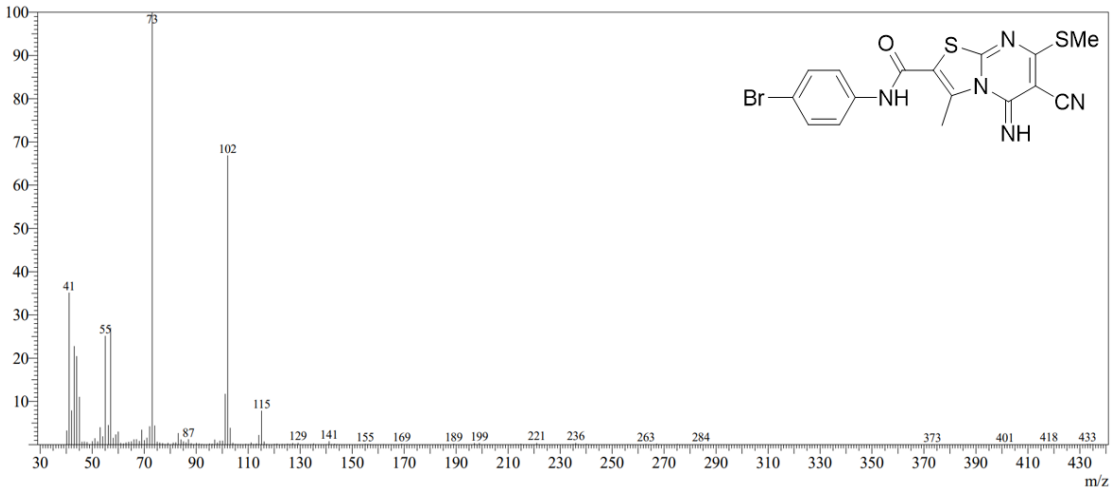

Fig. 22: Representative mass spectrum of compound CNTHNH-9

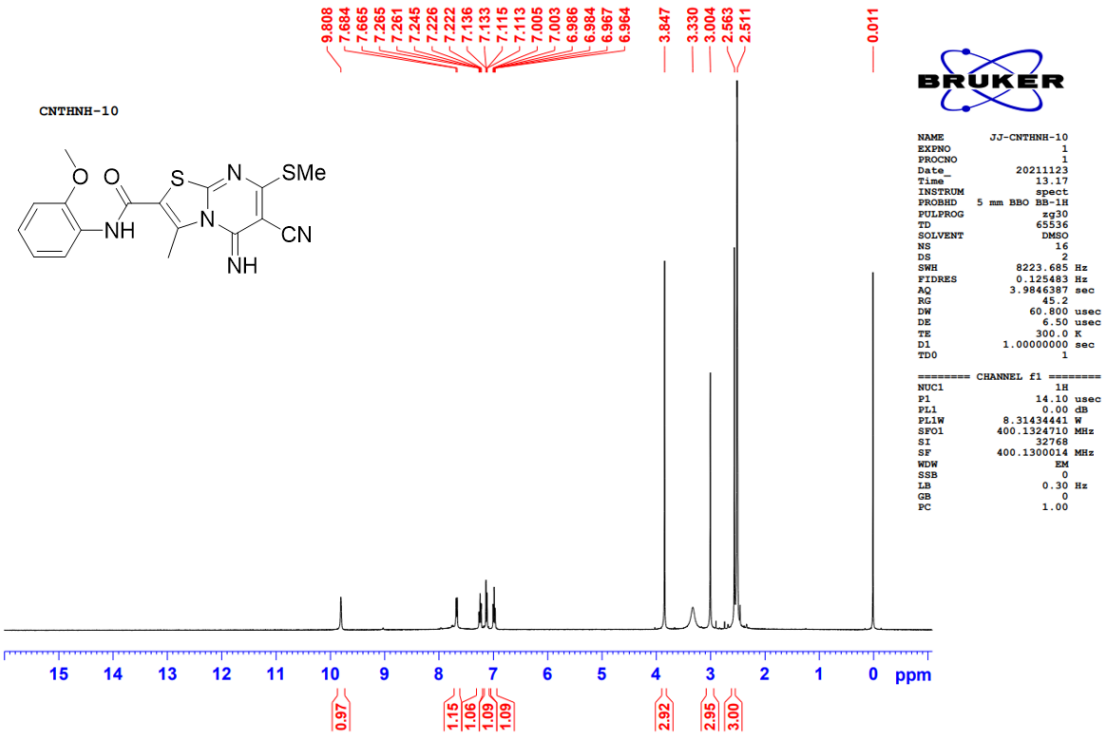

Fig. 23: Representative ^{1}H NMR spectrum of compound CNTHNH-10

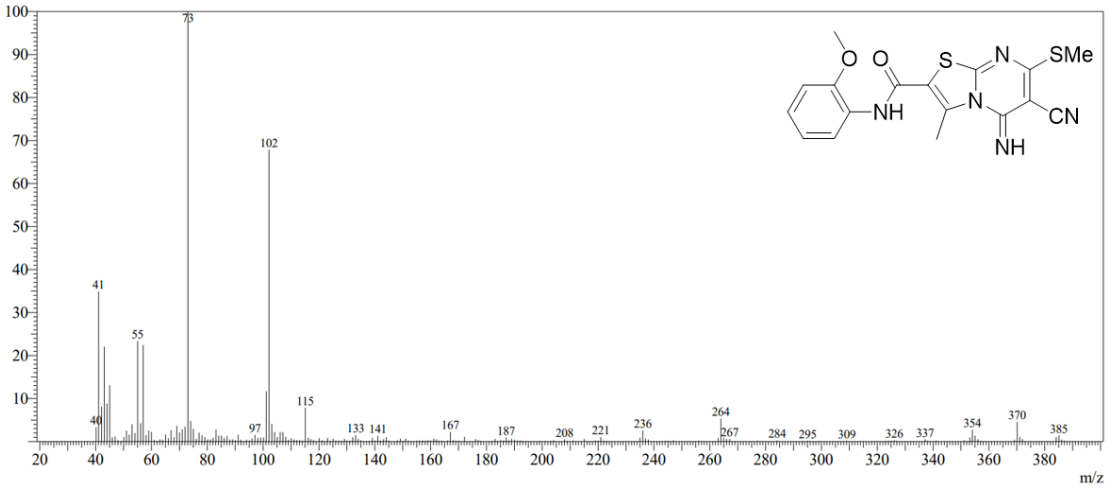

Fig. 24: Representative mass spectrum of compound CNTHNH-10

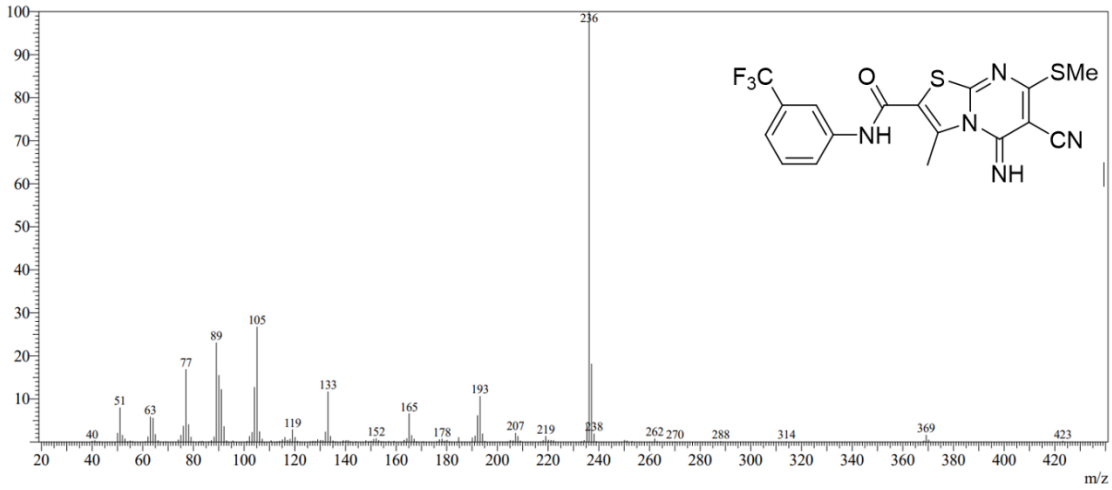

Fig. 25: Representative mass spectrum of compound CNTHNH-11

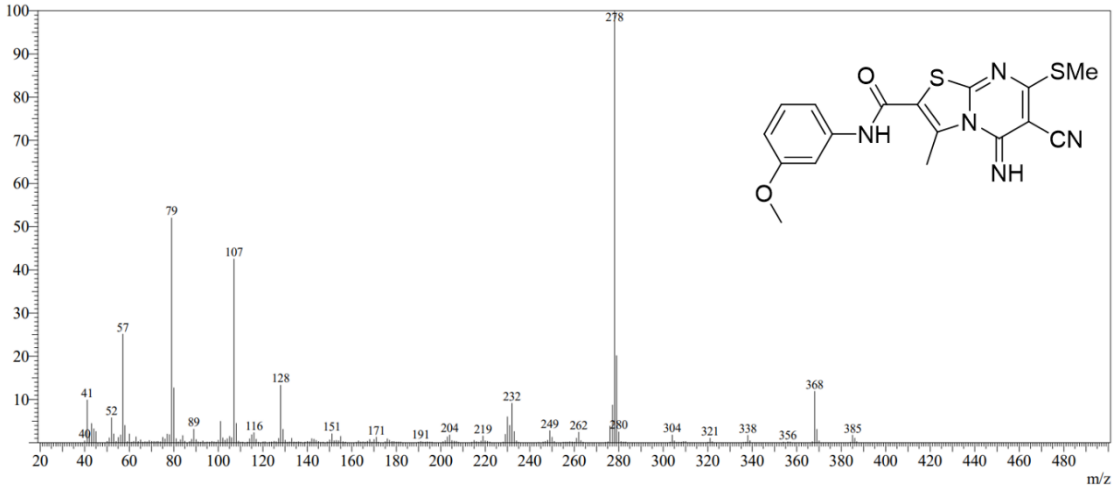

Fig. 26: Representative mass spectrum of compound CNTHNH-12

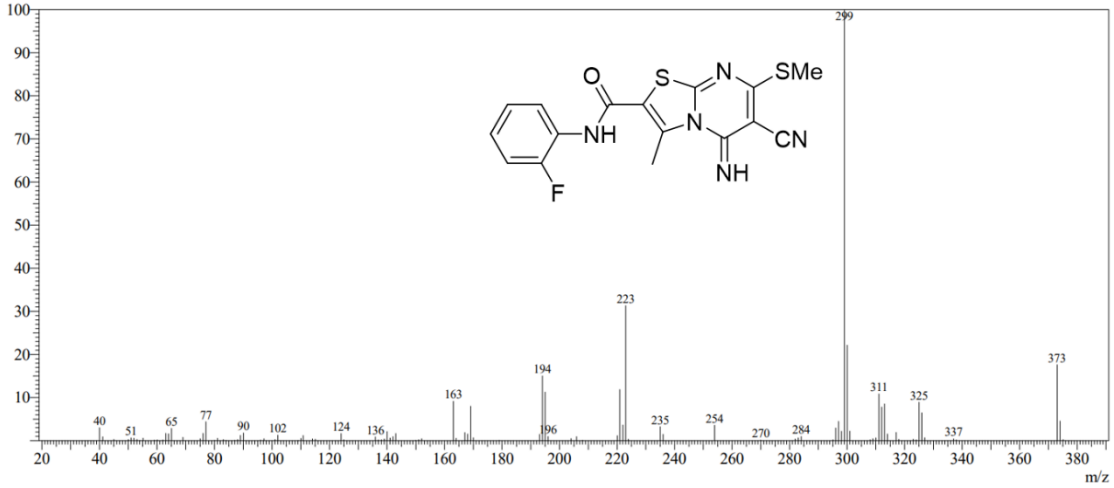

Fig. 27: Representative mass spectrum of compound CNTHNH-13

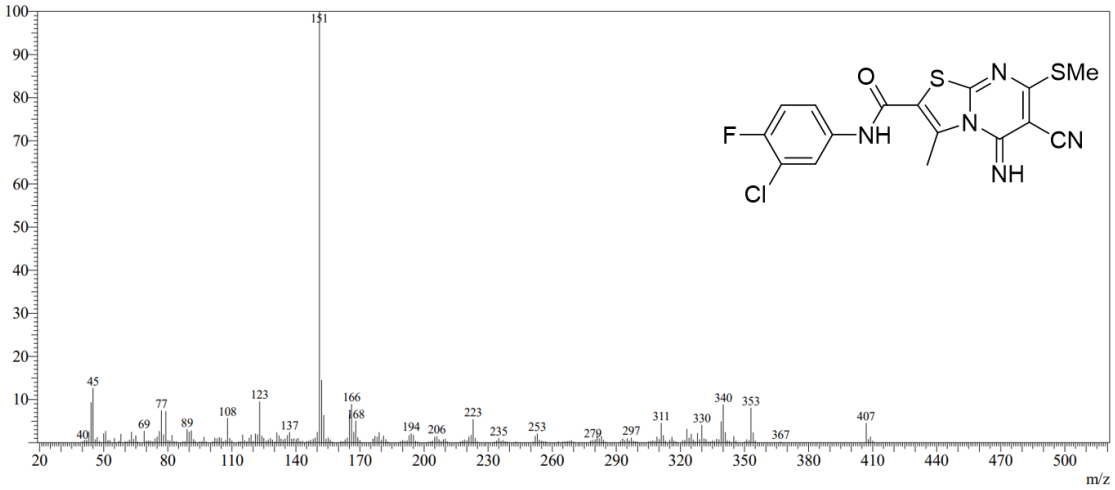

Fig. 28: Representative mass spectrum of compound CNTHNH-14

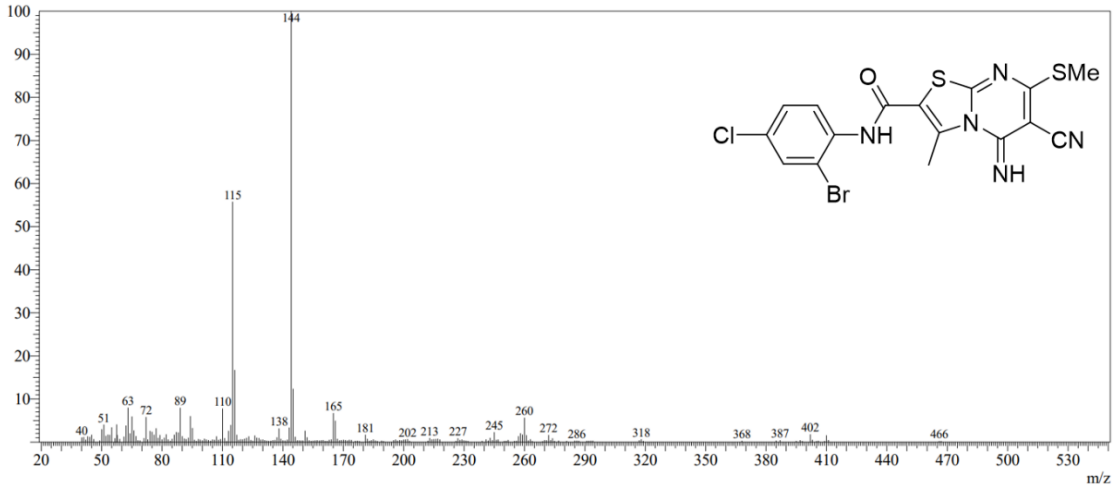

Fig. 29: Representative mass spectrum of compound CNTHNH-15